Cracking the dynamic code of the deep: Unexpected seasonal patterns of active protistan-bacterial microbiomes in the mesopelagic zone of the South China Sea

Ping Sun [a,b,*], Ying Wang [a,1], Xin Huang [a,1], SuSu Xu [a,1], Ramiro Logares [c], Yibin Huang [d,e,f], Dapeng Xu [f,g], Bangqin Huang [b,f,**]

[a] *Key Laboratory of the Ministry of Education for Coastal and Wetland Ecosystem, College of The Environment and Ecology, Xiamen University, Xiamen 361102, China*
[b] *Fujian Province Key Laboratory for Coastal Ecology and Environmental Studies, Xiamen University, Xiamen 361102, China*
[c] *Institute of Marine Sciences (ICM), CSIC, 08003 Barcelona, Catalonia, Spain*
[d] *Department of Ocean Sciences, University of California, Santa Cruz, CA 95064, USA*
[e] *National Oceanic and Atmospheric Administration, Pacific Marine Environmental Laboratory, Seattle, WA 98115, USA*
[f] *State Key Laboratory of Marine Environmental Science, College of Ocean and Earth Sciences, Xiamen University, Xiamen, China*
[g] *Institute of Marine Microbes and Ecospheres, College of Ocean and Earth Sciences, Xiamen University, Xiamen 361102, China*

ARTICLE INFO

ABSTRACT

Disentangling microbial dynamics in the mesopelagic zone is crucial due to its role in processing sinking photic production, affecting carbon export to the deep ocean. The relative importance of photic zone processes versus local biogeochemical conditions in mesopelagic microbial dynamics, especially seasonal dynamics, is largely unknown. We employed rRNA gene transcript-based high-throughput sequencing on 189 samples collected from both the photic and mesopelagic zones, along with seasonal observations, to understand the South China Sea's protistan-bacterial microbiota diversity, drivers, and mechanisms. Mesopelagic communities displayed unexpectedly greater seasonal but less vertical dynamics than photic counterparts. Temperature, dissolved oxygen, nutrients, and bacterial abundance drove mesopelagic communities vertically. Photic zone processes (using net community production and mixed layer depth as proxies) of past seasons, coinciding with strong monsoon periods, shaped seasonal fluctuations in mesopelagic communities, indicating a time-lag effect. Furthermore, certain microbes were identified as indicators for beta diversity by depth and season. This investigation deepens our understanding of how and why mesopelagic communities vary with season and depth. Recognizing the time-lagged effect of photic zone processes on mesopelagic communities is crucial for understanding the current and future configurations of the ocean microbiome, especially in the context of climate change and its effect on carbon export and ocean storage.

1. Introduction

The mesopelagic zone is typically defined as the layer between 200 m and 1,000 m of water depth where light can penetrate but is insufficient for photosynthesis to occur (Robinson et al., 2010). This zone plays a crucial role in the remineralization and repackaging of production sinking from the euphotic zone and has a profound effect on the efficiency of carbon transfer into the deep ocean (Buesseler et al., 2007).

Although far less is known about mesopelagic microbial communities than their photic counterparts, evidence is mounting that the mesopelagic zone is a unique reservoir of microbial diversity that is clearly distinct from its photic counterparts (Giner et al., 2020). Mesopelagic bacteria were found to have different community compositions than surface and deep chlorophyll maximum bacteria in local and global oceans (Delong et al., 2006; Sunagawa et al., 2015). The mesopelagic bacterial communities of oligotrophic oceans typically contained higher

---

proportions of Chloroflexi SAR202 (Morris et al., 2004), Deferribacteres SAR406 (Gordon & Giovannoni, 1996), and Deltaproteobacteria SAR324 (Wright et al., 1997) than their photic counterparts. Despite the fact that mesopelagic protists have been studied much less frequently than bacteria, previous research has revealed a distinct community composition of mesopelagic protists compared to their photic counterparts in the North Pacific Subtropical Gyre (Ollison et al., 2021), Southwest Pacific (Gutiérrez-Rodríguez et al., 2022), Eastern Tropical North Pacific (Duret et al., 2015), Ross Sea (Zoccarato et al., 2016), and the tropical and subtropical global oceans (Rigonato et al., 2023). Scuticociliatia (Sun et al., 2019), Radiolaria (RAD-C) (Giner et al., 2020) and the parasitic assemblage Syndiniales (Brown et al., 2009) are generally more prevalent in mesopelagic than photic zones. Even though prior research has increased our understanding of the microbiota in the mesopelagic zone, the resolution of community dynamics has been limited by the scope of data sets. For example, a few depth layers or sampling sites, which are rarely capable of illuminating the structured patterns of change that may occur with depth in mesopelagic zones. Therefore, accurately determining whether and how microbial communities vary with depth within the mesopelagic zone requires a substantial increase in sample collection, particularly at denser depth layers within this zone.

Besides the limited knowledge on the vertical variation of microbial communities within the mesopelagic zone, there is a lack of knowledge of the seasonal variation of these communities and the factors driving these changes in this zone. As the layer beneath the photic zone, the mesopelagic zone is subject to both continuous and episodic organic matter inputs from the photic zone (Robinson et al., 2010). Microorganisms, such as bacteria and protists, can attach to the surface of sinking particles and be transported to the mesopelagic zone, thereby altering the microbial community in this depth layer (Mestre et al., 2018; Duret et al., 2020). Analysis of samples collected from the Atlantic, Pacific, and Indian Oceans during the Malaspina expedition revealed that the prokaryotic community exhibits strong vertical connectivity, which is primarily mediated by particle sinking and dissolved organic matter, indicating that sinking particles and dissolved organic matter play a crucial role in determining the vertical distribution of prokaryotic communities (Mestre et al., 2018; Ruiz-González et al., 2020). According to Cram and colleagues (2015a, b), bacterial communities throughout the water column (from the surface to 890 m) at the San Pedro Ocean Time-Series Station (SPOTs) exhibit seasonality in relation to environmental conditions and/or microbial communities in the waters above. Protists and bacteria are responsible for the biogeochemical cycles in the mesopelagic zone, but seasonality studies of mesopelagic protists are rarely undertaken, with much of the focus on bacteria. Dolan et al. (2019) discovered that the community composition of tintinnid ciliates, phaeodarian radiolarians, and amphisolenid dinoflagellates in the mesopelagic layer (250 m) at the Point C station in Villefranche Bay, Mediterranean Sea, differed from that of the photic layer (30 m) and displayed clear seasonal patterns. In contrast, Blanco-Bercial et al. (2022) conducted a three-year sample collection at the Bermuda Atlantic Time-series Study (BATS) in the North Atlantic and determined that radiolarians dominated the protistan communities in the mesopelagic zone, with no discernible seasonal variation in community composition. In a similar manner, Ollison et al. (2021) investigated the mesopelagic protistan community at the ALOHA time-series station in the oligotrophic North Pacific Subtropical Gyre. They discovered that the dominant sequences of several taxonomic groups in the mesopelagic zones differed from those in the photic layer, indicating adaptation to the mesopelagic environment rather than passive migration from the photic zone community via sinking processes. This difference may have resulted from the lack of seasonality in the hydrological conditions, primary productivity, and particle flux measured throughout the year at the ALOHA time-series station in the North Pacific (Church et al., 2013). Understanding of mesopelagic community seasonal variations was previously based on observation

data from time-series stations in coastal regions, while knowledge of how dynamic these mesopelagic communities are and what organisms are transferred between seasons in the pelagic environment on a larger scale was rather limited. This is especially relevant when considering the heterogeneous nature of marine environments, in which microbes can vary on the scale of microns to millimeters (Long & Azam, 2001).

In addition, the mesopelagic is not a homogeneous layer but encompasses gradients in environmental parameters, including a rapid decrease in the sinking flux of particulate organic carbon, a decrease in light, temperature, and dissolved oxygen (DO), and an increase in hydrostatic pressure, salinity, and inorganic nutrients (Robinson et al., 2010). All of these physicochemical gradients can influence the distribution of the biota in this layer. Yet, there are clear knowledge gaps, such as those concerning microbial communities (Orsi et al., 2012; Duret et al., 2020). DO was found to play a crucial role in environmental filtering, which affected the distribution of mesopelagic bacteria in tropical and subtropical oceans (Rigonato et al., 2023), in the anoxic minimum oxygen zone (Ulloa et al., 2012), and in mesopelagic upwelled waters (Aldunate et al., 2018). In addition, even though interactions among mesopelagic microbial communities are among the least studied across marine habitats (St. John et al., 2016), results have shown that, similar to the surface ocean, microbial communities form complex interaction networks within the mesopelagic zones (Rigonato et al., 2023).

In the mesopelagic zone, microbial communities, primarily bacteria, re-mineralize over 70 % of particulate organic matter through heterotrophic processes (Friedlingstein et al., 2022). Grazing experiments revealed a strong predator–prey relationship between protists and bacteria in the mesopelagic zone, comparable to the photic zones in the Japan Sea (Cho et al., 2000), the Atlantic (Rocke et al., 2015), and the Mediterranean Sea (Pachiadaki et al., 2016). In the mesopelagic zones, strong associations between and among microbial communities are, therefore, expected. Collectively, the assembly of mesopelagic microbial communities can be regulated by photic zone processes and local biotic and abiotic variables. It is largely unknown to what extent the photic zone process versus local biogeochemical conditions influenced mesopelagic microbial communities.

In this study, we explored the dynamics of protistan-bacterial communities in the mesopelagic zone of the South China Sea (SCS). Our objectives were to determine whether mesopelagic protists and bacteria exhibited vertical and seasonal variations, and if so, what is the relative influence of photic zone processes versus local biogeochemical conditions on these microbial dynamics. Due to the export of particulate organic carbon (POC) from the photic zone to the mesopelagic zones, we hypothesized that fluctuations in net community production (NCP) and mixed layer depth (MLD) would be related to variations in mesopelagic communities and that the influence of photic zone processes would diminish with increasing depths in the mesopelagic zone. Additionally, given the predominance of bacteria in POC processing within the mesopelagic zone (Steinberg et al., 2008), we expected the photic zone process to have a greater impact on mesopelagic bacteria than on protists.

2. Materials and methods

2.1. Sampling

A total of 189 samples were collected from 16 sites across the basin of the South China Sea, spanning a spatial range of 111.97°E–118.50°E and 10.02°N–20.76°N (Table S1; Fig. 1A). The samples covered nine water depths (surface, DCM (Deep Chlorophyll Maximum), 100 m, 200 m, 300 m, 400 m, 600 m, 800 m, and 1,000 m) and were taken during two distinct seasons, spring and fall, to account for the strong seasonality of photic zone processes and their potential influence on mesopelagic communities. The seasonal sampling occurred between April 19th and May 10th and September 3rd and 26th, 2020 (Table S1; Fig. 1A). In this
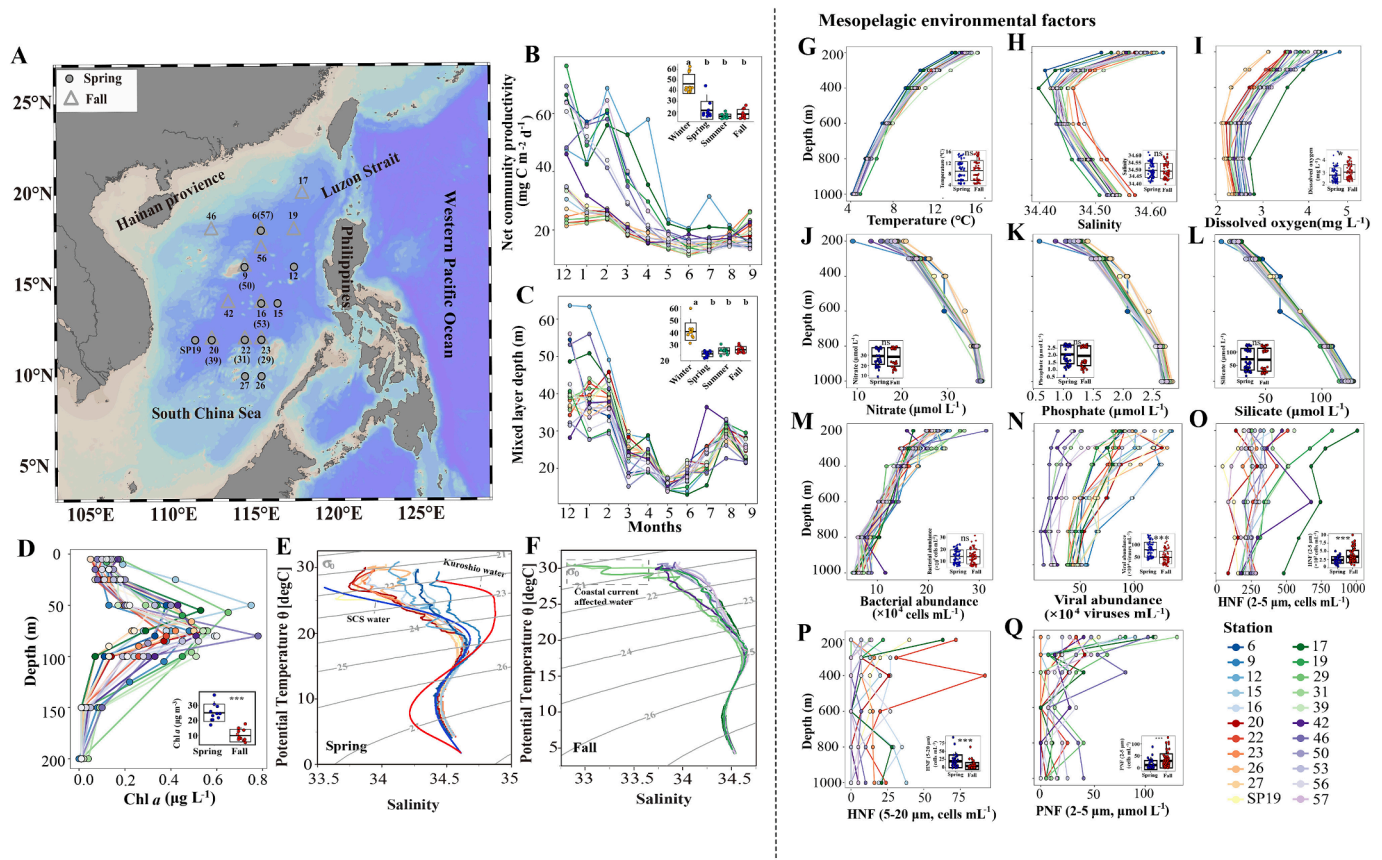
Fig. 1. A Map of the South China Sea with field sampling stations highlighted. **B, C** The net community production (NCP) and mixed layer depth (MLD) for the sampling stations. Since photic zone processes continuously influence the mesopelagic zone and may have time-lag effects on mesopelagic communities, we included the NCP and MLD of the sampled months and the five months preceding them, which covered seasons with marked NCP and MLD differences. **D-F** The chlorophyll *a*, potential temperature (θ, °C) vs. salinity for the sampling stations in spring and fall. The colored dots indicate the different sampling stations. **G-Q** The profiles of temperature, salinity, dissolved oxygen, nutrients, and abundances of bacteria, viruses, HNF, and PNF with respect to depth in mesopelagic zones for the sampling stations. The colored lines represent the sampling stations, while the colored circles represent the sampling depths. HNF (2–5 μm), HNF (5–20 μm), and PNF (2–5 μm), size-fractioned heterotrophic nanoflagellate (HNF) and pigmented nanoflagellate (PNF) across the size ranges of 2–5 μm and 5–20 μm.

study, the potential influencing factors on mesopelagic microbial communities, such as photic zone processes (representing organic loading), water masses, and local biogeochemical factors (such as temperature, salinity, DO, nutrients, bacterial and viral abundances, and the ratio of heterotrophic nanoflagellates abundance to bacterial abundances (as a proxy for grazing pressure on bacteria)) were evaluated. Hydrodynamic profiles for depth, temperature, salinity, and dissolved oxygen were measured using an onboard automatic observing system (SeaBird Electronics SBE43). The temperature, salinity, and dissolved oxygen of the CTD are validated by the National Center of Ocean Standards and Metrology, and the data are processed using the SBE Processing Data software (v7.22) according to the "Specifications for Oceanographic Survey". A water sample ranging from 500 to 1,000 ml for chlorophyll *a* (Chl *a*) analysis was filtered through 25 mm GF/F glass fiber filters (Whatman, UK; under a vacuum pressure less than 100 mm Hg) and then immediately frozen in liquid nitrogen prior to analysis in the laboratory. In the laboratory, the filters were submersed in 90 % acetone in the dark at −20 °C for 16–24 h. The concentrations of Chl *a* extracted into the acetone were measured with a Trilogy fluorometer (Turner Designs, USA) at a wavelength of 436 nm, as outlined by Parsons et al. (1984). The concentrations of nitrate, phosphate, and silicate were determined using an AA3 nutrient automatic analyzer (SEAL Analytical, Germany) following the procedure described by Du et al. (2013). The detection limits for dissolved inorganic nitrogen (nitrate plus nitrite), phosphate (PO_4^{3-}), and silicate ($Si(OH)_4$) were 0.03 μmol/L, 0.03 μmol/L, and 0.05 μmol/L, respectively. To count nanoflagellates, 50 ml of seawater was

filtered using a 20 μm nylon mesh to remove larger plankton. The filtered sample was then fixed with a final concentration of 1 % ice-cold glutaraldehyde and stained with DAPI (4′,6-diamidino-2-phenylindole; Sigma, USA) for 10 min. The nanoflagellates were finally quantified using fluorescence microscopy (Nikon ECLIPSE 90i, Nikon, Japan) based on the method described by Sherr et al. (1993). When exposed to UV-excitation, the nuclei of nanoflagellates exhibited a blue fluorescence, which facilitated the differentiation of cells from non-living debris. Subsequently, when exposed to blue light excitation, nanoflagellates that demonstrated red fluorescence were classified as pigmented nano-flagellates (PNF); those nanoflagellates lacking red fluorescence were identified as heterotrophic nanoflagellates (HNF). For bacterial and viral abundance analyses, 1.8 ml of a 20 μm-prefiltered sample was fixed with ice-cold glutaraldehyde at a final concentration of 1 % for 15 min in the dark, flash-frozen in liquid nitrogen, and stored at −80 °C. Bacterial and viral abundances were analyzed using a flow cytometer (Epics Altra II, Beckman Coulter). For bacterial abundance analysis, samples were thawed at 37 °C in the laboratory and then stained with SYBR green I (1/10,000 final concentration) in the dark for 15 min at room temperature. Then, 10 mL fluorescent microspheres (diameter of 1 μm; 10^5/mL; Molecular Probes, Eugene, OR, USA) were added to the 1 mL dyed samples as an internal standard. The samples were run at a flow rate of 0.1 to 1 mL/h. The enumeration of bacterial abundance followed (Marie et al., 1999). Heterotrophic bacteria were identified in the plots of red fluorescence versus green fluorescence. For viral abundance analysis, samples were thawed at 37 °C and diluted 5 to 50 times with Tris-EDTA

buffer (pH 8; Sigma-Aldrich). Then, the samples were stained with SYBR green I (1/20,000 final concentration), heated at 80 °C for 10 min in the dark, and cooled for 5 min before analysis. The samples were measured using an Epics Altra II flow cytometer (Beckman Coulter, USA) with an emitted wavelength of 488 nm, a collection rate of 0.1–1 mL h-1, and a sampling time of 100 s. The enumeration of viral abundance followed (Brussaard, 2004). To distinguish small viral particles from noise signals in the flow cytometer, we primarily rely on the green fluorescence (GFL) signal from nucleic acid staining. This is complemented by cellular parameters such as cell size (forward-scattered light) and cellular granularity (side-scattered light).

Here, we used remotely sensed net community production (NCP, a metric of photic layer carbon export potential (Emerson, 2014)) and mixed layer depth (MLD, obtained from a hydrographic model (HYCOM)) as proxies for the photic zone process to assess its impact on mesopelagic microbial communities. MLD is used to represent upper-ocean mixing processes that may have a crucial impact on net primary production by regulating the availability of light and nutrients to the phytoplankton as well as carbon export to mesopelagic zones, such as enhanced DOC export by physical mixing (Hansell & Orellana, 2021) and enhanced POC export through mixed layered pump (Dall'Olmo et al., 2016). Because the mesopelagic zone is continuously influenced by photic zone processes, we included not only the NCP and MLD of the sampled months but also those of the five months preceding the sampling month, which accounted for nearly the entire sampled year. The MLD was derived from hydrographic model output data (HYCOM, http://orca.science.oregonstate.edu/1080.by.2160.monthly.hdf.mld125.hycom.php), which is defined as the depth with the density threshold of 0.03 kg m^{-3} relative to the 10 m reference depth. The NCP was calculated using the following formula as a product of remotely sensed net primary production (NPP) and empirically estimated carbon export ratio (e-ratio) developed by Laws et al. (2011).

$$NCP = NPP*\underbrace{0.04756*(0.78 - 0.43*T/30)*NPP^{0.307}}_{e-ratio}$$

where T represents the temperature of the seawater. Satellite-retrieved NPP from the vertically Generalized Production Model (VGPM) was chosen because it is the most commonly used model (Behrenfeld & Falkowski, 1997), which is accessible at http://sites.science.oregonstate.edu/ocean.productivity.

2.2. Extraction and PCR

Microbial cells were collected by filtering 8 L of seawater from each station through 0.22 μm pore-size polycarbonate filters (47 mm diameter, Merck Millipore, USA) with a peristaltic pump at < 200 mm Hg. The filters were kept at −80 °C before the extraction of nucleic acids. Given that environmental DNA can persist for an extended period of time in marine environments (Dell'Anno & Corinaldesi, 2004) and that dormant cells could represent a substantial proportion of marine microbial cells (Zinger et al., 2012), we used a rRNA gene transcript-based approach to investigate the active microbial communities in the mesopelagic zones. Polycarbonate filters were cut into small pieces and subjected to bead beating to allow mechanical lysis. A commercial extraction kit, the RNeasy Mini Kit (Qiagen, USA), was used for RNA extraction. All extraction steps were performed according to the manufacturer's instructions. The RNase-free DNase set (Qiagen, Germany) was used to remove the remaining DNA from the RNA extracts. RNA was immediately reverse transcribed to cDNA using a High-Capacity cDNA Reverse Transcription Kit (Applied Biosystems, USA) as described by the kit protocol. The protistan community was profiled by targeting the V4 region of the 18S rRNA gene transcript using the eukaryote-specific primers TAReuk454FWD1 (5′-CCAGCASCYGCGGTAATTCC-3′) and TAReukREV3 (5′-ACTTTCGTTCTTGATYRA-3′) (Stoeck et al., 2010). Primers 341F (5′-CCTAYGGGRBGCASCAG-3′) and 806R (5′-

GGACTACNNGGGTATCTAAT-3′) were used to amplify the V3-V4 region of the 16S rRNA gene transcript (Roggenbuck et al., 2014). PCR conditions were described previously (Stoeck et al., 2010; Roggenbuck et al., 2014). Each sample was amplified in triplicate, pooled, and purified using the Wizard SV Gel and PCR Cleanup System Kit (Promega, USA). Paired-end sequencing of the amplicons from cDNA templates was performed using the Illumina MiSeq PE300 sequencing platform by Majorbio Bioinformatics Technology Co. Ltd. (Shanghai, China).

2.3. Sequencing data processing

Sequences were mainly processed with USEARCH v10 (Edgar, 2013) and QIIME v1.9.0 (Caporaso et al., 2010). The same pipeline was applied for both protistan 18S and bacterial 16S rRNA gene transcript sequences. Sequences were quality-checked using Trimmomatic v0.38 (Bolger et al., 2014) and FLASH v1.2.11 (Magoč & Salzberg, 2011), and the details followed Sun et al. (2023). After quality control, chimera detection and singleton removal were carried out with USEARCH v10. After removing chimeras and singletons, the final curated reads were clustered into operational taxonomic units (OTUs) at 97 % identity using USEARCH v10. The representative sequences of OTUs were blasted against the Protist Ribosomal Reference Database v4.11.1 (PR2) (Guillou et al., 2012) and SILVA v132 (Quast et al., 2012) using assign_taxonomy.py in QIIME v1.9.0. For the protistan community, an OTU table was randomly rarefied to 13,244 sequences after non-protistan OTUs (e.g., metazoans and fungi) had been filtered out. For the bacterial community, an OTU table was randomly rarefied to 28,306 sequences after nonbacterial OTUs (e.g., archaea and chloroplasts) had been filtered out. These corresponded to a minimum number of reads per sample for protistan and bacterial communities.

2.4. Statistical analyses

All statistical analyses as well as the production of figures were carried out with R (version 3.6.1, https://r-project.org/) unless otherwise noted. Alpha diversity indices were calculated for each sample using QIIME v. 1.8.0. For alpha diversity analysis, nonparametric tests (Wilcox rank-sum test for two groups and Kruskal-Wallis test for multiple groups) were used, and the results were drawn by the "boxplot" package in R. The ordination of the communities from the 189 samples was visualized with a Principal Coordinate Analysis (PCoA) plot using the "Vegan" package in R (Oksanen et al., 2010). Analysis of similarity (ANOSIM) with 9,999 permutations was used to further statistically assess between-group differences. The photic zone processes (i.e., NCP and MLD of both previous and current seasons of the samplings) and local biogeochemical factors (i.e., temperature, salinity, DO, nutrients, bacterial and viral abundances, and the ratio of heterotrophic nanoflagellates abundance to bacterial abundances) were used to predict the microbial vertical (using the PCoA 1 as the proxy) and seasonal (using the PCoA 2 as the proxy) variations. The investigation was carried out using the "randomForest" package (Breiman et al., 2018). Random forest models containing 1,000 trees were trained using 100 repeats of 10-fold cross-validation, and the amount of variables sampled at each node was optimized. The "rfPermute" package (Archer, 2021) was used to determine the importance of each predictor (in this case, photic zone processes, local biotic and abiotic variables) for the response variables.

We excluded OTUs with a relative abundance of less than 0.01 % to mitigate biases associated with the presence of rare species. Subsequently, we employed the Kruskal-Wallis test and Bonferroni correction ('kruskal.test' function from the "stats" package in R) to identify differential OTUs with relative abundances that were significantly enriched in each depth strata and each season. For our statistical analysis, the nine water depths were stratified into three distinct depth zones: the photic zone (surface to 100 m depth), the upper mesopelagic zone (200 m to 400 m depth), and the lower mesopelagic zone (600 m to 1000 m depth). The OTUs exhibiting a significantly higher abundance ($P < 0.05$) in the

upper mesopelagic zone were classified as upper mesopelagic-enriched OTUs. Conversely, OTUs with a significantly higher abundance ($P <$ 0.05) in the lower mesopelagic zone were designated as lower mesopelagic-enriched OTUs. The OTUs with significantly ($P < 0.05$) greater relative abundance in photic samples were classified as photic-enriched OTUs, while the remaining OTUs with no significant differences in relative abundance were classified as 'Others'. Those OTUs with significantly higher abundance in mesopelagic zones but showing an insignificant difference between upper and lower mesopelagic samples were categorized as mesopelagic ubiquitous OTUs. In a similar way, we identified significantly ($P < 0.05$) enriched OTUs in the spring and fall for both protists and bacteria. OTUs with significantly higher abundance in the spring were grouped as spring-enriched OTUs, whereas those with significantly higher abundance in the fall were categorized as fall-enriched OTUs, and the remaining OTUs with no significant differences in relative abundance were categorized as 'Others'.

A co-occurrence network was constructed to determine the relationships between protists and bacteria. To reduce noise and complexity in the network analysis, OTUs with a relative abundance of less than 0.01 % and detected in fewer than 30 % of samples were eliminated from the study. The "Hmisc" package was used to calculate the Spearman's rank coefficient (r) between the remaining OTUs. The network analysis took into account correlations that were both robust ($|r| \geq 0.6$) and statistically significant (false discovery rate-corrected P-values < 0.01). To visualize networks and perform modular analysis, we used the interactive Gephi v0.9.2 (Bastian et al., 2009) and the package circlize (Gu et al., 2014).

3. Results

3.1. Sampling region

The South China Sea is subjected to strong seasonal monsoons, thereby generating seasonal variations in NCP and MLD (Fig. 1B, C). The NCP decreased sharply from winter (Dec., Jan., Feb.) to spring (Mar., Apr., May), remained relatively stable during summer (June, July, Aug.), and increased slightly in fall (Sep.) (Fig. 1B). The MLD decreased sharply from winter to spring and remained relatively stable during summer and fall (Fig. 1C). These trends align with the established higher NCP and deeper MLD in winter, and the lower NCP and shallower MLD in summer for the SCS. The seasonal variations in NCP and MLD mirror the reported shifts in the flux of Particulate Organic Carbon (POC) in this region, endorsing the idea that both NCP and MLD are intricately tied to the transfer of organic matter from the photic waters to the mesopelagic zone, as supported by the previous studies (Li et al., 2017). Additionally, our measurements of chlorophyll *a* in the photic zone show notable differences between depth layers (surface, DCM, and bottom of photic zone) and seasons (spring versus fall) (Fig. 1D). Specifically, the chlorophyll *a* concentration was highest at DCM in comparison to the other depth layers, and it was also higher in spring than in summer (Fig. 1D). These findings illustrate the complex interplay between primary productivity and oceanic conditions across different times of the year in the South China Sea. Temperature and salinity measurements at spring sampling stations showed a mixture of SCS and Kuroshio water in the northeast stations, with this influence primarily affecting waters above 80 m depth (i.e., stations 6, 9, 12, 15, and 16) (Fig. 1E). For the fall sampling, temperature and salinity data from the southernmost stations (i.e., stations 29, 31, 39, and 42) showed the presence of coastal currents, which were characterized by their distinctively higher temperatures and lower salinities compared to the typical oligotrophic conditions of the basin (Fig. 1F). Contrasting the photic zone, where multiple water masses were present, a relative homogeneity was observed in the mesopelagic zone across all stations regarding temperature and salinity (Fig. 1E-H). The analysis of abiotic variables within the mesopelagic zones revealed a general increase in nutrient concentrations such as nitrate, phosphate, and silicate with depth, while

temperature and DO exhibited a declining trend. Salinity decreased with depth between 200 and 400 m and increased with depth between 400 and 800 m, indicating a halocline within mesopelagic zones (Fig. 1G-L). The biotic factors, including abundance of viruses, bacteria, and size-fractioned heterotrophic nanoflagellate (HNF) and pigmented nano-flagellate (PNF) across the size ranges of 2–5 μm, 5–10 μm and 10–20 μm displayed a general decrease with depth within the mesopelagic zones (Fig. 1M-Q). Notably, HNF in the 2–5 μm size range dominated the nanoflagellate community in the mesopelagic zone. The ratio of HNF (2–5 μm) to bacterial abundances, serving as a proxy for grazing pressure, was significantly higher between depths of 600 and 1,000 m than between depths of 200 and 400 m (Wilcox rank-sum test, p < 0.001) (Fig. S1).

3.2. Dynamics of mesopelagic protistan-bacterial microbiota

In this study, the relative abundance of assemblages within the community is evaluated based on relative read abundance rather than cell count. Approximately 91 % of the protistan sequences were assigned to Dinophyta (41.7 %), Stramenopiles (20.6 %), Ciliophora (17.4 %), and Rhizaria (11.4 %), demonstrating the prevalence of these four protistan assemblages in the water columns of the South China Sea basin (Fig. 2A). Dinophyta (mainly Dinophyceae) were prevalent in the water column, and their relative read abundance was slightly higher in mesopelagic zones than in photic zones, with the greatest relative read abundance occurring in the upper mesopelagic zone (Fig. 2A). The relative read abundance of Dino-Group I and II of the parasitic assemblage Syndiniales increased from photic to mesopelagic zones, with a nearly balanced distribution between upper and lower mesopelagic zones (Fig. 2A). The relative read abundance of the Stramenopiles assemblage Pelagophycea (mainly Pelagomonadales) was significantly higher in the photic zone than in the mesopelagic zone (Wilcox rank-sum test, p < 0.001), whereas the relative read abundance of the Bicoecea (mainly Anoecales) was highest in the lower mesopelagic zone (Fig. 2A). Distribution patterns of the ciliate assemblages Spirotrichea and Oligohymenophorea (primarily Scuticociliatia) exhibited distinct trends with depth, with relative read abundance of the former decreasing from photic to mesopelagic zones and relative read abundance of the latter increasing in the upper mesopelagic zone (Fig. 2A). Rhizaria assemblage Acantharea exhibited a greater relative read abundance in photic than mesopelagic zones (Fig. 2A), whereas assemblage RAD-B exhibited the opposite trend (Fig. 2A). Other protistan assemblages contributed less than 9 %.

Approximately 80 % of the total bacterial communities in the water columns consisted of Gammaproteobacteria (30.5 %), Alphaproteobacteria (26.3 %), Oxyphotobacteria (15.0 %), and Deltaproteobacteria (8.7 %) (Fig. 2B). Oxyphotobacteria (mainly Synechococcales) were significantly more prevalent in photic than mesopelagic communities (Wilcox rank-sum test, p < 0.001), whereas the Gammaproteobacteria assemblages Alteromonadales and Oceanospirillales demonstrated the opposite trend, with the highest relative read abundance occurring in the lower mesopelagic zone (Fig. 2B). The relative read abundance of Alphaproteobacteria assemblages SAR11 clade, Rhodospirillales, and Rickettsiales decreased from photic to mesopelagic zones (Fig. 2B), whereas Sphingomonadales and Rhodobacterales exhibited the opposite trend, with the highest relative read abundances occurring in the lower mesopelagic zone. Actinobacteria (5.4 %) (primarily assemblage Acidimicrobiia) and Chloroflexi (4.1 %) (primarily assemblage SAR202 clade) were more prevalent in the mesopelagic zone than in the photic zone, with a balanced distribution between the upper and lower mesopelagic zones (Fig. 2B). Bacteroidetes (3.7 %) and Marinimicrobia (SAR406 clade) (2.9 %) contributed more to the mesopelagic zone than the photic zone (Fig. 2B), with the highest relative read abundance occurring in the upper mesopelagic zones. Other bacterial assemblages constitute a small proportion of the community.

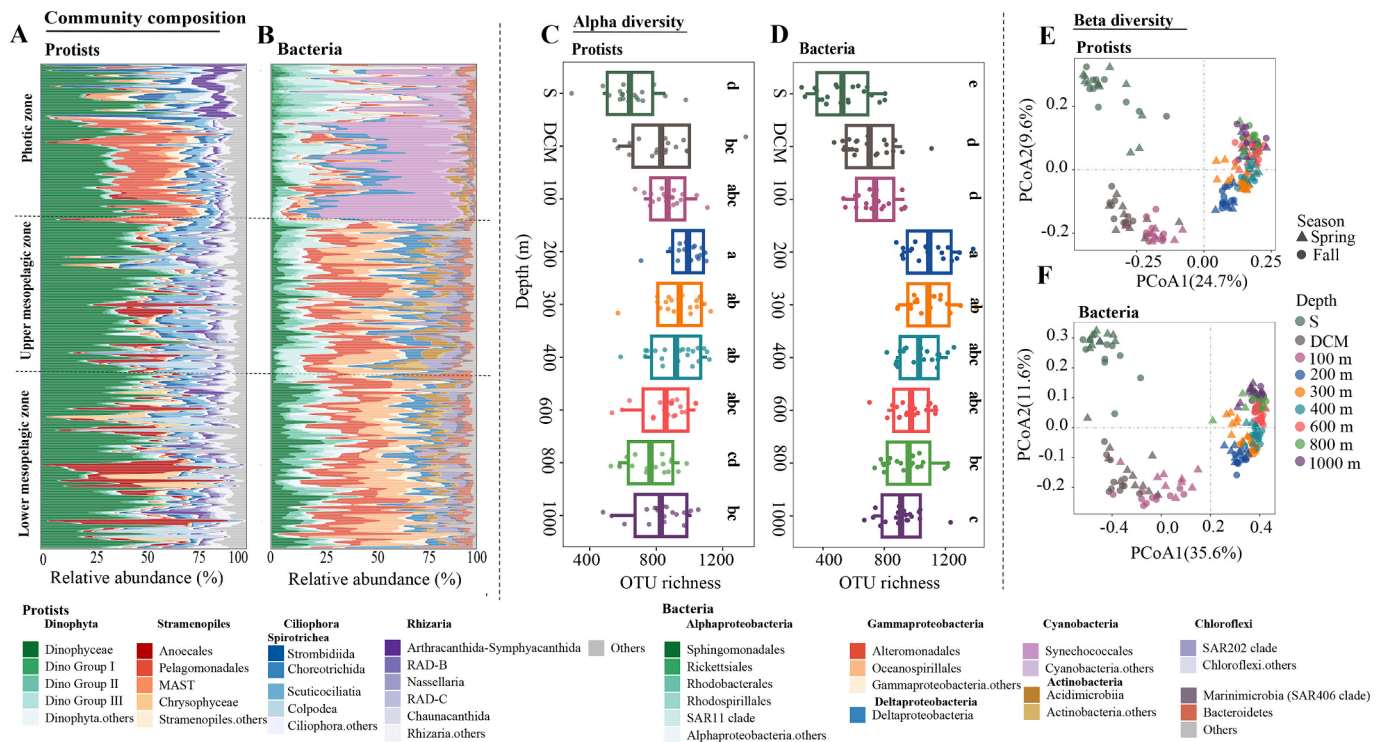Analyses of alpha diversity revealed that upper mesopelagic

Fig. 2. Overview of community composition, alpha- and beta-diversity of protists and bacteria in the water column of the South China Sea. **A, B** Alluvial diagram showing the relative read abundance of protistan and bacterial phyla or classes. Despite the application of rRNA-gene transcript-based sequencing, it is essential to recognize that certain organisms, such as Dinophyceae, with multiple gene copies and a high DNA content per cell, may still be selectively favored, leading to an imbalanced overrepresentation.**C, D** Boxplot of the alpha-diversity of protistan and bacterial communities among different depth layers. **E, F** Principal coordinate analysis (PCoA) profile of protistan and bacterial diversity across all samples using the Bray-Curtis dissimilarity metric.

contained a greater diversity of OTUs than lower mesopelagic (Wilcox rank-sum test, p < 0.05), with the peak of alpha diversity occurring at the 200 m layer, a result that was consistent across both protistan and bacterial communities as well as various alpha diversity indices (Fig. 2C, D, S2A-J). Significant seasonal differences in the alpha diversity of mesopelagic protists and bacteria were also observed (Fig. S2K-P; Wilcox rank-sum test, all p < 0.05, except for the Shannon index for bacteria). In addition, we used Principle Co-ordinate Analysis (PCoA) to investigate the differences between microbial communities based on Bray-Curtis dissimilarities (Fig. 2E, F). The clustered groups clearly corresponded to the respective vertical zones, namely the photic and mesopelagic zones, which are identical for protists and bacteria (Fig. 2E, F). Examining the mesopelagic zone revealed the vertical subdivision of community composition along axis 1 (PCoA 1) and the seasonal subdivision along axis 2 (PCoA 2), especially for the bacterial community (Fig. 3A, B). ANOSIM also confirmed the significance of depth (protists, R = 0.608, P < 0.001 (Permutation Test); bacteria, R = 0.563, P < 0.001 (Permutation Test)) and seasonality (protists, R = 0.231, P < 0.001 (Permutation Test); bacteria, R = 0.422, P < 0.001 (Permutation Test)) on mesopelagic microbial communities (Table S2). Comparing upper and lower mesopelagic zones independently, seasonal effects became more pronounced as zones transitioned from upper to lower (Fig. S3; Table S2).

3.3. Drivers of mesopelagic microbial communities

We applied the Random Forest (RF) model to identify factors influencing the distributions of protistan and bacterial communities in the mesopelagic zone, incorporating variables related to photic zone processes and local biogeochemical conditions. To reduce multicollinearity among environmental factors, we conducted separate principal component analyses (PCAs) for physicochemical factors, nutrients, and photic zone processes of the previous season. The first principal

components from these PCAs (PCA1.tdo (temperature and DO), PCA1. nps (nitrate, phosphate, and silicate), and PCA1.np (NCP$_{PS}$ and MLD$_{PS}$)) were used as predictors in the random forest analysis to explore vertical and seasonal variations in mesopelagic microbial communities. The results of Random Forest indicated that the vertical variation of mesopelagic protists and bacteria (using PCoA1 in PCoA as the proxy, Fig. 3A, B) was primarily the result of local biogeochemical conditions (Fig. 3C, D). The seasonal variations of mesopelagic protists and bacteria (using the PCoA2 as a proxy, Fig. 3A, B) were primarily driven by the NCP and MLD of the previous rather than current sampling season, corresponding to the strong seasonal monsoon periods in SCS (Fig. 3E, F).

3.4. Identifying key taxa associated with mesopelagic dynamics

Since mesopelagic microbial communities exhibited pronounced compositional differences across depths and seasons, we examined which OTUs were specific to different depth layers (i.e., upper and lower mesopelagic) and to different seasons (spring and fall). We used the Kruskal-Wallis test to determine differences in OTU relative abundance between depth layers and seasons (Fig. 4). Upper (148 for protists; 112 for bacteria) and lower (99 for protists; 74 for bacteria) mesopelagic microbial communities contained 260 and 173 distinct OTUs, respectively (Fig. 4A; Table S3-S4). Similarly, seasonally different OTUs were identified for mesopelagic protists (258 for spring and 42 for fall) and bacteria (140 for spring and 150 for fall) (Fig. 4B; Table S3-S4). These vertically differentiated OTUs represented 20.7 % and 32.5 %, respectively, of the mesopelagic protistan and bacterial community sequences. These seasonally different OTUs accounted for 72.9 % and 60 %, respectively, of the mesopelagic protistan and bacterial community sequences. Both protists and bacteria exhibit patterns that resemble the depth and season effects observed in analyses of community structure (Fig. 3A, B). The three assemblages Syndiniales, Dinophyceae (Dinophyta), and Scuticociliatia (Ciliophora) comprised the greatest number
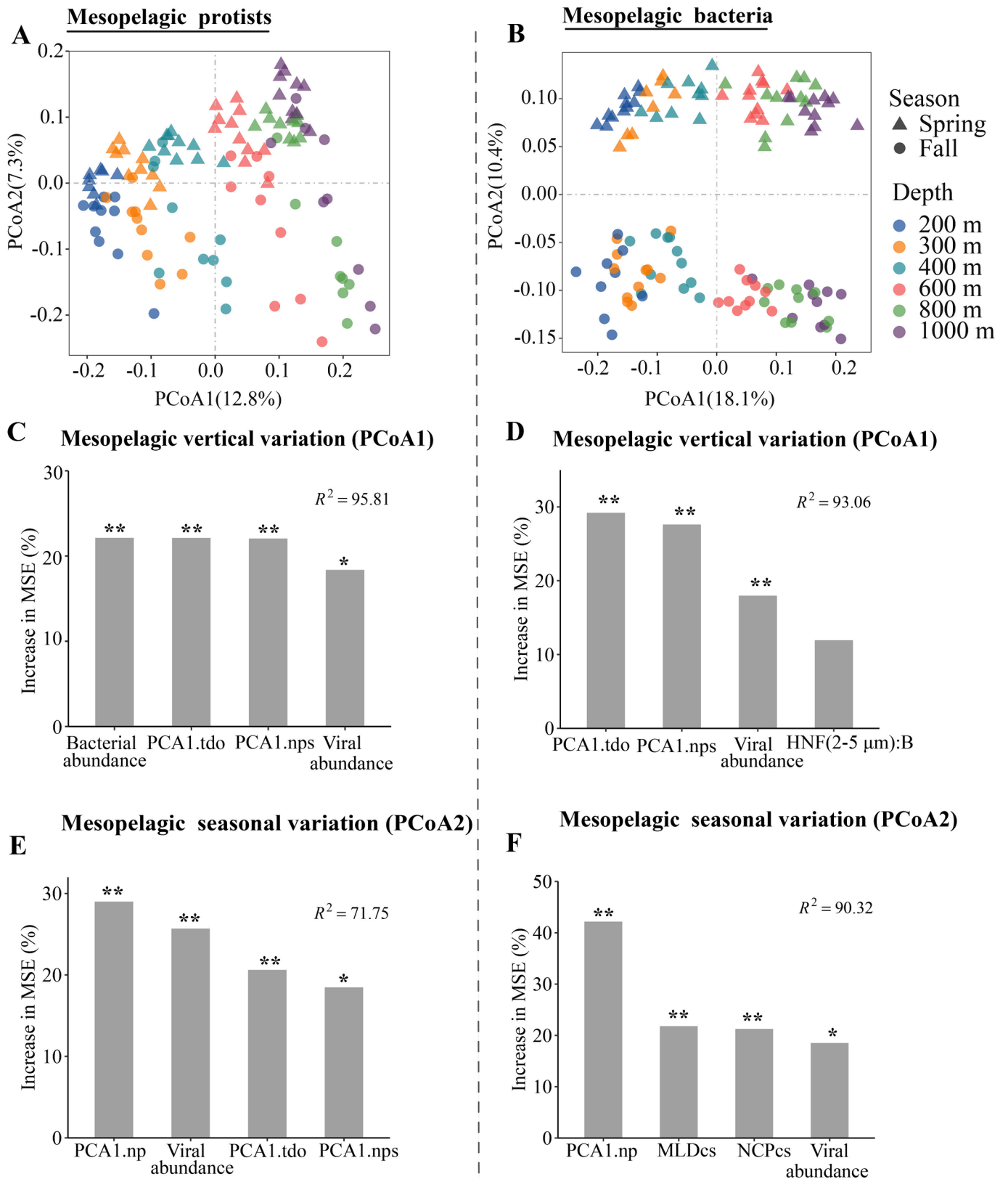
Fig. 3. The beta-diversity and drivers of protistan and bacterial communities in the mesopelagic zone of the South China Sea. **A, B** Principal coordinate analysis (PCoA) profile of mesopelagic protistan and bacterial diversity using the Bray-Curtis dissimilarity metric. **C-F** The predictions of photic zone processes (using NCP and MLD as proxies) and local biogeochemical conditions for the vertical (using PCoA1 in A and B as proxies) and seasonal (using PCoA2 in A and B as proxies) variation of mesopelagic protists and bacteria based on random forest regression analysis. HNF(2–5 μm):B, the ratio of heterotrophic nanoflagellates abundance to bacterial abundances; NCP_{ps}, net community production of the current season; MLD_{cs}, mixed layer depth of the current season; PCA1.tdo, PCA1.nps, and PCA1.np, the first principal components of a PCA of physiochemical factors (temperature and DO), a PCA of nutrients (nitrate, phosphate, and silicate), and a PCA of photic zone processes of the previous season, respectively.
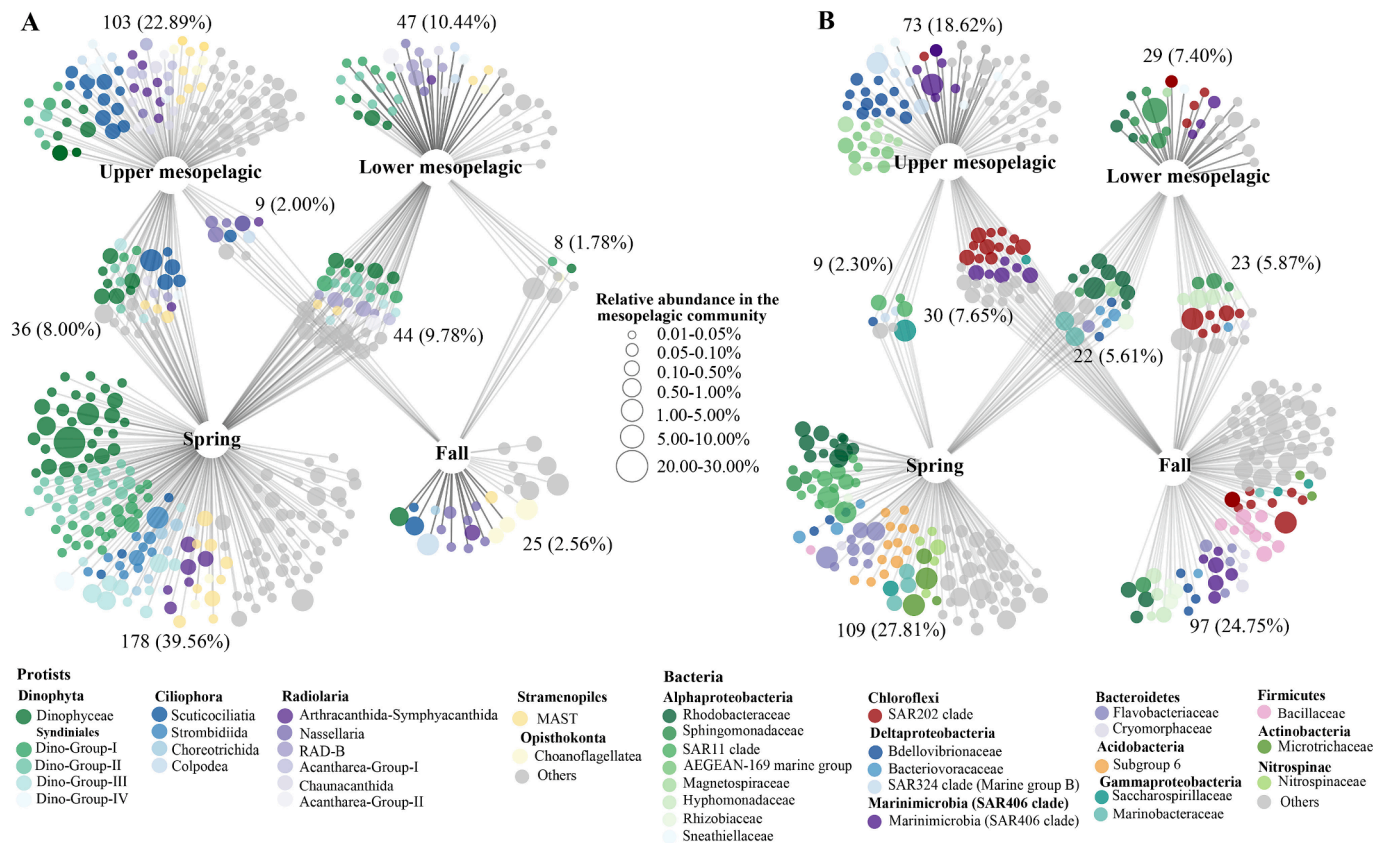
Fig. 4. Bipartite networks display vertically and seasonally differential OTUs in mesopelagic protistan and bacterial communities. **A** The set of mesopelagic protistan OTUs assigned to classes or orders was observed to be significantly different between depth layers and seasons. **B** The set of mesopelagic bacterial OTUs assigned to classes or families was observed to be significantly different between depth layers and seasons. Upper and lower mesopelagic refer to samples collected in the upper (including samples collected from water depth between 200 m and 400 m) and lower (including samples collected from water depth between 600 m and 1,000 m) mesopelagic zones, respectively; spring and fall represent samples collected in the spring and fall, respectively.

of vertically differential OTUs and were responsible for the greatest number of mesopelagic protistan community sequences (Fig. 4A; Table S3). The identification of the seasonally different OTUs revealed a comparable taxonomic pattern for mesopelagic protists (Fig. 4A). For mesopelagic bacteria, the majority of vertically different OTUs are associated with SAR202 (Chloroflexi), followed by Bdellovibrionaceae (Deltaproteobacteria), Marinimicrobia (SAR406clade), and Rhodobacteraceae (Alphaproteobacteria) (Fig. 4B; Table S4). Seasonally different OTUs of mesopelagic bacteria were primarily associated with the SAR202 (Chloroflexi), Rhodobacteraceae (Alphaproteobacteria), SAR11 clade (Alphaproteobacteria), and Flavobacteriaceae (Bacteroidetes) (Fig. 4B; Table S4). Despite the similarity in the differential assemblages between depths and seasons at class and order/family levels, there is little overlap at the OTU level for the vertically and seasonally differential OTUs, indicating a set of specific vertical and seasonal OTUs for mesopelagic microbial communities (Fig. 4; Table S3).

3.5. Co-occurrence pattern of protistan and bacterial communities

Lastly, we explored the extent to which depth and season impacted co-occurrence patterns in microbial communities by mapping depth-layered and seasonal differential OTUs into the total microbial networks. We found that three modules (M1-M3) contained relatively high proportions of depth-layered differential OTUs in the network, whereas seasonal differential OTUs dispersed across modules. The differential OTUs associated with the photic zone predominantly clustered in M1, distinctly separated from M2, which primarily encompassed differential OTUs from the upper mesopelagic zone (Fig. 5A, B). M3 was

distinguished from the other two modules (M1 and M2) by mainly containing differential OTUs specific to the lower mesopelagic zone as well as OTUs ubiquitous across mesopelagic depths (Fig. 5A, B).

In details, M1 (photic zone) displayed a relatively balanced number of protistan and bacterial OTUs (protists 55.5 %; bacteria 44.5 %), with major contributions from the protistan assemblages of Stramenopiles and Ciliophora and the bacterial assemblages of Alphaproteobacteria, Cyanobacteria, and Deltaproteobacteria in terms of edge numbers (Fig. 5C-G). Conversely, M2 (upper mesopelagic) was characterized by a predominance of bacterial OTUs (protists 14.0 %; bacteria 86.0 %), with notable representation from Deltaproteobacteria, Alphaproteobacteria, Chloroflexi, and Marinimicrobia (SAR406 clade), as evidenced by their numbers of edges within the module (Fig. 5C-G). M3 (lower mesopelagic and mesopelagic ubiquitous), in contrast, was primarily composed of protistan OTUs (protists 81.1 %; bacteria 18.9 %), with the assemblages Syndiniales and Rhizaria dominating in terms of their proportion of edges within the module (Fig. 5C-G).

The major contributors to protist-bacteria associations varied across different depth layers. In M1 (photic zone), the dominant associations are primarily between the protistan assemblages of Ciliophora (mainly Spirotrichea and Oligohymenophorea) and Stramenopiles (mainly MAST and Bacillariophyta) and the bacterial assemblages of Alphaproteobacteria (mainly Rhodospirillales), Gammaproteobacteria (SAR86 clade), Deltaproteobacteria (SAR324 clade) and Cyanobacteria (mainly Synechococcales) (Fig. 5H). Moving to M2 (upper mesopelagic), the main associations shift towards protistan assemblages of Ciliophora (mainly Scuticociliatia) and Dinophyceae, and bacterial assemblages including Marinimicrobia (SAR406 clade), Deltaproteobacteria (mainly Bdellovibrionales) and Alphaproteobacteria (mainly Rhodospirillales)
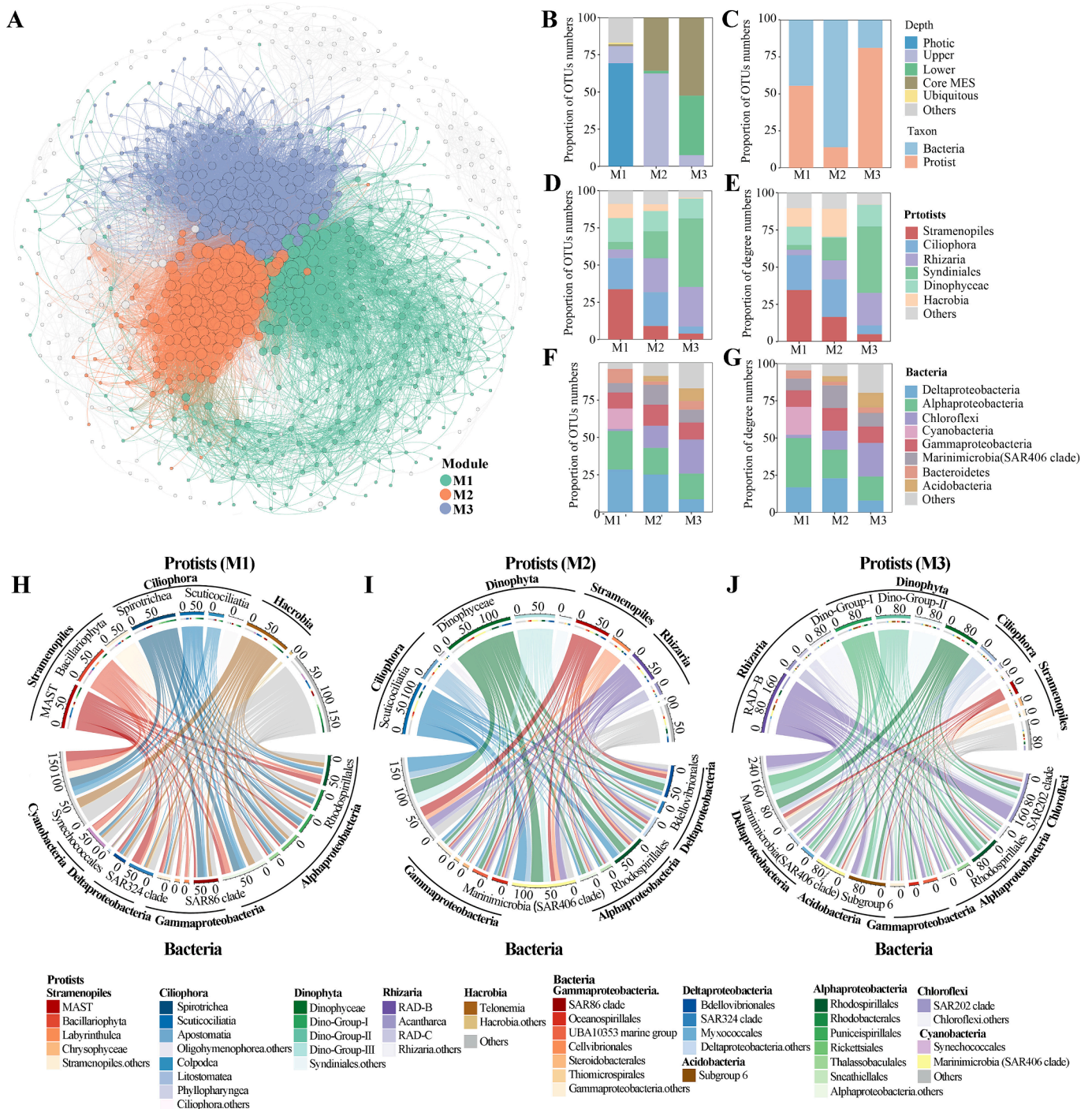
Fig. 5. **A** A Co-occurrence network of protistan and bacterial communities revealing the modular associations between microbial OTUs. **B, C** Histograms illustrating the proportion of depth-differential OTUs and the distribution of protistan and bacterial OTUs across modules I-III, respectivly. **D-G** Histograms illustrate the composition of major protistan and bacterial assemblages, detailing both the proportion of OTUs and the proportion of degrees within each module. **H-J** Chord diagrams depicting the interactions between protists and bacteria in each module, highlighting assemblages with their degree contributions being at least 1%, with the thickness of each ribbon reflecting the frequency of co-occurrence.

(Fig. 5I). In M3 (lower mesopelagic and mesopelagic ubiquitous), the prevalent associations are between protistan assemblages of Rhizaria (mainly RAD-B) and Syndiniales (mainly Dino-Group-I and II) and bacterial assemblages of Chloroflexi (SAR202 clade), Alphaproteobacteria (Rhodospirillales), Acidobacteria (mainly subgroup 6), and Marinimicrobia (SAR406 clade) (Fig. 5J).

4. Discussion

4.1. Vertical distribution of mesopelagic protists and bacteria

We observed a distinct vertical distribution pattern for both mesopelagic protists and bacteria (upper and lower mesopelagic), which is driven primarily by local biogeochemical conditions, including temperature, dissolved oxygen, nutrients, and bacterial abundance. This

indicated that the factors driving the vertical distribution patterns of microbial communities in mesopelagic zones may be similar across taxa, although their relative importance may differ to some extent (Fig. 3C, D). Protists and bacteria are subject to various direct and indirect temperature-related effects. It has been demonstrated that temperature affects the metabolism of microbes (Sarmento et al., 2010). Specifically, it increases the growth rates of protists and bacteria by stimulating their metabolism (Boscolo-Galazzo et al., 2018). Sinking particles are progressively re-mineralized by heterotrophic bacteria as they sink through the mesopelagic zones (Buesseler et al., 2007), and water column temperature, together with POC density and ballasting with minerals or organic polymers, deeply influences bacterial respiration (Laws et al., 2000). In other circumstances, however, the direct metabolic response may be more complex than a simple increase in abundance due to a temperature rise; it may also result from the taxa's thermal optimum and realized temporal thermal niches (Trombetta et al., 2021). Also, temperature can indirectly affect protists and bacteria via prey-predator (Delaney, 2003) and/or parasite/symbiont-host interactions (Arandia-Gorostidi et al., 2017).

DO was found to be a key factor in determining the importance of mesopelagic protists and bacteria. In agreement with our findings, the Oxygen Minimum Zone (OMZ) has revealed a great deal about the effect of DO on mesopelagic protistan and bacterial communities (Wright et al., 2012; Giner et al., 2020). This demonstrated the crucial role of DO in both OMZ and non-OMZ mesopelagic communities. The sinking of POC to mesopelagic depths is understood to result in a high abundance of organic matter, which is consumed and respired by heterotrophic organisms, such as heterotrophic bacteria and heterotrophic protists, involving oxygen consumption. Although our study does not include direct measurements of POC and dissolved organic carbon (DOC), this understanding aligns with established biogeochemical principles and previous investigations (Steinberg et al., 2008; Shea et al., 2023). Consequently, it is possible, based on the physiological properties of bacteria and protists, that the metabolic processes of bacteria and protists are influenced by the statistically significant lower oxygen conditions in the mesopelagic zones than in the photic zones (average 5.31 mg/L in the photic zone vs. average 2.89 mg/L in the mesopelagic zones in the present study, Wilcox rank-sum test, $p < 0.001$). For example, low dissolved oxygen has also been identified as a crucial factor influencing regional transfer efficiency in the mesopelagic zone (Lam et al., 2011).

The observed correlation between inorganic nutrients such as nitrate, phosphate, and silicate, and the vertical distributions of mesopelagic protists and bacteria in this study may not necessarily denote a causal relationship between the nutrient profiles and microbial vertical variations. Inorganic nutrients are largely depleted in the photic zone, yet are re-mineralized and released into the mesopelagic water through microbial processes, resulting in a relatively high abundance of these nutrients in mesopelagic regions (Orcutt et al., 2011). This suggests that the vertical community structuring of mesopelagic protists and bacteria, delineated as upper versus lower mesopelagic communities, could potentially play a pivotal role in nutrient cycling. Specifically, by recycling inorganic nutrients from organic matter that sinks from the photic zones, these microbial communities may substantially influence the nutrient dynamics within the mesopelagic zone.

Besides those of the above physiochemical factors, the notable effect of bacterial abundance on mesopelagic protists observed in this study may be partially attributed to predator–prey interactions. Pernice et al. (2015) found that bacterial abundance was a key variable in explaining the variance of mesopelagic heterotrophic protistan abundance, suggesting a potential predator–prey relationship between protists and bacteria. Indeed, in-situ grazing experiments suggested that mesopelagic protistan communities might exhibit comparable or even enhanced bacterial grazing activities relative to their photic zones counterparts, despite the general trend of decreasing abundance with depth (Rocke et al., 2015; Pachiadaki et al., 2016). The observed ratio of HNF to bacterial abundances, employed as a proxy for grazing pressure in this

study, highlights the role of grazing in shaping the vertical distribution of mesopelagic bacteria. Our simultaneous observations of protistan and bacterial communities revealed that their associations varied between depth layers within mesopelagic zones. This variation underscored the depth-dependent complexity of ecological relationships within the mesopelagic zones. In this study, scuticociliates played a key role in protist-bacteria interactions within the upper mesopelagic zones. These ciliates are particularly abundant in habitats with high levels of organic matter, nutrients, and bacteria, and their crucial role in changing prey community structure through grazing (Šimek et al., 1997; Urrutxurtu et al., 2003), are further supported by Sun et al. (2019), who found that scuticociliates dominated the ciliate community in the mesopelagic zones of the north SCS. Additionally, the prevalence of mixoplanktonic Dinophyceae taxa in mesopelagic zones indicated a diverse ecological interaction pattern, contributing to the complexity of predator–prey dynamics in the western Pacific Ocean and the Sargasso Sea (Sun et al., 2023; Zhao et al., 2022; Blanco-Bercial et al., 2022). The metabolic activity and preference for lower mesopelagic zones by heterotrophic RAD groups like RAD-B (Flegontova et al., 2023; Gutiérrez-Rodríguez et al., 2022) and the significance of SAR202 and SAR406 as free-living bacteria in aphotic zones (Salazar et al., 2016) suggest shifts in microbial community composition, potentially reflecting changes in predatory pressures. Moreover, the association between Syndiniales and bacteria such as Alphaproteobacteria and Chloroflexi may indicate a cycle of eukaryotic host cell lysis leading to dissolved organic matter release, driving bacterial activity in a manner akin to the viral shunt (Jephcott et al., 2016).

In the present study, RF also revealed the significance of viruses on the vertical distribution of mesopelagic protistan and bacterial communities. This may be the result of a viral control in the protistan and bacterial communities (Tanaka et al., 2004; Yamada et al., 2018). In addition, a recent single-cell genomics study on protists suggests that protists, particularly Picozoa and Choanozoa, may graze on free-living viral particles (Brown et al., 2020). Therefore, the relationship between protists and viruses may result from a combination of viral shunting, and trophic linkage, or the consumption of viruses.

4.2. Seasonal dynamics of mesopelagic protists and bacteria

In the present study, we observed a more pronounced seasonal pattern in mesopelagic microbial communities than in photic microbial communities (Fig. S3), with the trend becoming more pronounced as the mesopelagic zones transitioned from upper to lower. Given that many of local environmental factors were relatively stable across the sampling seasons (Fig. 1G-Q), we hypothesize that photic zone processes could explain the majority of seasonal variation in mesopelagic microbial communities. We refer to POC flux (using NCP as a proxy) and physical conditions (using MLD as a proxy) in the photic zones as photic zone processes. We hypothesize that the mesopelagic microbial communities would exhibit pronounced differences in response to strong (such as winter and spring) or weak (such as summer and fall) NCP and deep (such as fall and winter) or shallow (such as spring and summer) MLD in the photic zones, and that the magnitude of these effects would diminish with increasing mesopelagic depths. Considering that the mesopelagic zone is continuously influenced by photic zone processes and that photic zone processes might present time-lag impacts on the mesopelagic communities as described before (Cram et al., 2015a, b; Li et al., 2018), we therefore included not only the NCP and MLD of the sampled months but also those of the five months preceding the sampling month, which covered the seasons that exhibited notable differences in photic zone processes, such as NCP and MLD. RF results corroborate our hypothesis that revealed the importance of the NCP and MLD of the previous season (corresponding to winter and summer, which are monsoon periods in SCS), not the current season of sampling, on seasonal variations of mesopelagic communities, which explains the more pronounced seasonal pattern observed in mesopelagic than in photic communities

(Fig. S3). This may result from the fluctuating amount and composition of POC throughout the seasons and its slow sinking rate in the SCS (Yang et al., 2022). A seven-year time-series study on mesopelagic biogenic flux revealed a clear seasonal variation in flux and a markedly higher flux during monsoon periods, particularly during the northeastern monsoon period (winter) in the central SCS (Li et al., 2017). In addition, a study on POC by ^{234}Th in the SCS reveals that ^{234}Th is predominantly carried by small sinking particles (70–80 % of the total) in the northern South China Sea (SCS), representing the majority sinking of ^{234}Th (Hung et al., 2012). This corresponded well with the study based on ten years of investigation of phytoplankton communities in SCS, which found that pico- and nano-sized phytoplankton dominated the basin of SCS (Xiao et al., 2018). Small particles are found to be less effective at carbon transfer than large particles with ballast, such as diatoms, and are easily disintegrated into suspended particles (Duret et al., 2020). A recent study on POC sinking in the mesopelagic waters of the South China Sea has confirmed this. Yang et al. (2022) collected samples of sinking POC using sediment traps and free-drifting sediment traps and measured the carbon fluxes and attenuation rates of POC. They estimated that the average sinking velocity of particles in the SCS was 15 ± 9 m per day, indicating that slow-sinking particles largely contributed to the POC flux in the SCS and that the mesopelagic zone acted as a substantial sink for slow-sinking POC. In conclusion, our study demonstrated that seasonal variations in mesopelagic microbial communities in the South China Sea are primarily influenced by photic zone processes, particularly NCP and MLD from the previous season. While we focused on POC dynamics, the role of DOC in shaping mesopelagic communities should not be overlooked. However, due to the lack of DOC measurements in the present study, a discussion of DOC dynamics is not included in this study. Future research integrating both POC and DOC measurements would offer a more complete picture of microbial dynamics in the mesopelagic zone.

4.3. Vertical and seasonal signatures of mesopelagic protists and bacteria

This study revealed that the mesopelagic zone is home to a unique subset of vertically and seasonally distributed protists and bacteria. Our finding of differential OTUs belonging to the Syndiniales, Dinophyceae, and Scuticociliatia contributed most to the vertical and seasonal patterns of mesopelagic protistan communities, which is in line with the previous observations in the South China Sea, Western Pacific Ocean, and global oceans (de Vargas et al., 2015; Sun et al., 2019, 2023; Zhao et al., 2022). The Syndiniales are a diverse group of parasitic dinoflagellates that infect a wide range of marine organisms, such as metazoans, radiolarians, ciliates, and even other dinoflagellates (Guillou et al., 2008). This group is widespread in the ocean, and a global ocean survey found that Syndiniales are a major contributor to heterotrophic protists in mesopelagic zones (de Vargas et al., 2015). Additionally, Syndiniales kill their host, which results in the release of free-living parasitic dinospores (Guillou et al., 2008), which may also contribute to the high diversity of Syndiniales in mesopelagic zones. Seasonal variation in POC composition and flux as well as the relatively larger cell size of dinoflagellates compared to other phytoplankton in oligotrophic oceans, which makes it easier for them to sink toward the deep oceans (Durkin et al., 2016), may contribute to the differential seasonal distribution of mesopelagic Dinophyceae. In addition, numerous members of the Dinophyceae possess heterotrophic and mixotrophic metabolic traits that enable them to consume microbes and organic matter and parasitize other plankton (Guillou et al., 2008), allowing them to tolerate or survive in this twilight environment. Using a method based on rRNA gene transcripts, the present study determined that Dinophyceae are metabolically active, suggesting that these organisms may either inhabit the mesopelagic zone or may exhibit a heterotrophic and/or mixotrophy nutrition mode when sinking from the photic zone to mesopelagic zones. Scuticociliates (Ciliophora) are abundant in habitats with high levels of organic matter, nutrients, and bacteria (Urrutxurtu et al., 2003). The vertical variation in the distribution of particulate organic carbon (POC) and bacterial abundance within mesopelagic zones may be associated with the differential distribution of Scuticociliates between depths.

Our finding of differential OTUs belonging to the SAR202 clade (Chloroflexi) contributed the most to the number of vertically and seasonally differential OTUs of mesopelagic bacteria. SAR202 bacteria, which belong to the phylum Chloroflexi, are free-living, heterotrophic bacterioplankton that are abundant in mesopelagic waters (Morris et al., 2004). The SAR202 lineage includes at least five subclades with distinct ecological profiles (Thrash et al., 2017), and the best-known examples are those of SAR202 subclades III and V from mesopelagic zones, which can encode multiple families of oxidative enzymes involved in the oxidation of recalcitrant dissolved organic matter (Landry et al., 2017). Shotgun metagenomic and metatranscriptomic methods identified CAZy (carbohydrate-active enzyme) genes in SAR202 genomes, implicating them in the degradation of complex compounds such as chitin and pectin (Thrash et al., 2017). The emerging picture of metabolic potentials in SAR202 indicates the group has a highly flexible genetic potential for the degradation of organic matter, which is consistent with the fact that detritus is a major energy source in mesopelagic zones (Yilmaz et al., 2016). The large proportion of overlapping in vertically and seasonally differential OTUs of SAR202 indicated that the SAR202 cluster is well adapted to the prevailing environmental conditions in the mesopelagic zones and may have contributed a substantial proportion of mesopelagic bacterial activity.

In our dataset, another noteworthy group of differential OTUs belonged to the Bdellovibrionaceae family, with dynamics predominantly driven by the OM27 clade. This clade comprises unculturable bacteria phylogenetically related to Bdellovibrio (Orsi et al., 2016). OM27 is reported to be a protein-degrading, particle-attached bacterium capable of preying on Gram-negative bacteria by infiltrating and occupying the periplasmic space between the inner and outer membranes of its prey (Fuchs et al., 2005). The increased abundance of OM27 in the upper mesopelagic zone might be atrributable to the high concentrations of particulate organic carbon (POC) in this region, providing a plentiful source of prey for these predatory bacteria.

The SAR406 clade, another prominent group of differential OTUs, was among the first bacterial groups detected below the euphotic zones using 16S rRNA gene sequencing (Fuhrman et al., 1993). This clade is ubiquitously distributed and displays a depth-dependent increase in relative abundance, with its presence in the mesopelagic zone being approximately five times higher than in the surface waters (Yilmaz et al., 2016). Previous studies in the deep North Atlantic Ocean have linked SAR406 to refractory dissolved organic matter (DOM) compounds (Guerrero-Feijóo et al., 2017). Genomic analyses reveal that the SAR406 clade possesses the genetic potential for complex carbohydrate turnover and anaerobic respiratory processes (Thrash et al., 2017). The notable presence of SAR406 in the mesopelagic zone, particularly in these low-light environments, may be attributed to its importance in the turnover of organic matter and its contribution to the microbial dynamics in this region.

5. Limitations of the study

While our study employed rRNA gene transcript-based sequencing to investigate mesopelagic microbial communities, it is important to recognize that certain organisms, such as Dinophyceae, with multiple gene copies and a high DNA content per cell may still be selectively favored, leading to an imbalanced overrepresentation. Another point to consider is that our research is based on samples collected over two seasons within a single year (2020). While this provides valuable insights into seasonal dynamics, it may not fully encompass the potential interannual variability in these microbial communities. Therefore, extending the study to include multi-year sampling could offer a more comprehensive understanding of the temporal patterns in mesopelagic microbial communities.

6. Conclusion

We present a conceptual framework to characterize the distribution of composition, alpha- and beta diversity, and drivers of mesopelagic protistan and bacterial communities in a marginal sea oligotrophic system (Fig. 6). Our study reveals the occurrence of protistan and bacterial communities that vary vertically and seasonally not only in the photic zone but also in the mesopelagic zone, as well as the organisms driving these vertical and seasonal changes. In addition, we demonstrate that the drivers responsible for the vertical and seasonal dynamics of mesopelagic protists and bacteria, that is, local biogeochemical factors shaped the vertical distribution while photic zone processes of the previous season, primarily the ones during seasonal monsoon periods, drove the seasonal dynamics of mesopelagic microbial communities. This research increased our understanding of whether and why mesopelagic protists and bacteria exhibit vertical and seasonal dynamics, highlighting the crucial role of the time-lag effect of photic zone processes in the seasonal dynamics of mesopelagic microbial communities, with implications for carbon export and long-term storage in the oceans.

7. Data accessibility

All the sequencing sequences for 18S and 16S rRNA genes from this study have been deposited in the public NCBI Sequence Read Archive (SRA) database under BioProject accession number PRJNA983541.

CRediT authorship contribution statement

Ping Sun: Writing – review & editing, Writing – original draft, Visualization, Supervision, Formal analysis, Data curation, Conceptualization. **Ying Wang:** Writing – original draft, Formal analysis, Data curation. **Xin Huang:** Writing – original draft, Investigation, Formal analysis, Data curation. **SuSu Xu:** Investigation, Data curation. **Ramiro Logares:** Writing – review & editing. **Yibin Huang:** Writing – review & editing, Data curation. **Dapeng Xu:** Writing – review & editing, Writing – original draft, Formal analysis, Conceptualization. **Bangqin Huang:** Writing – review & editing, Conceptualization.
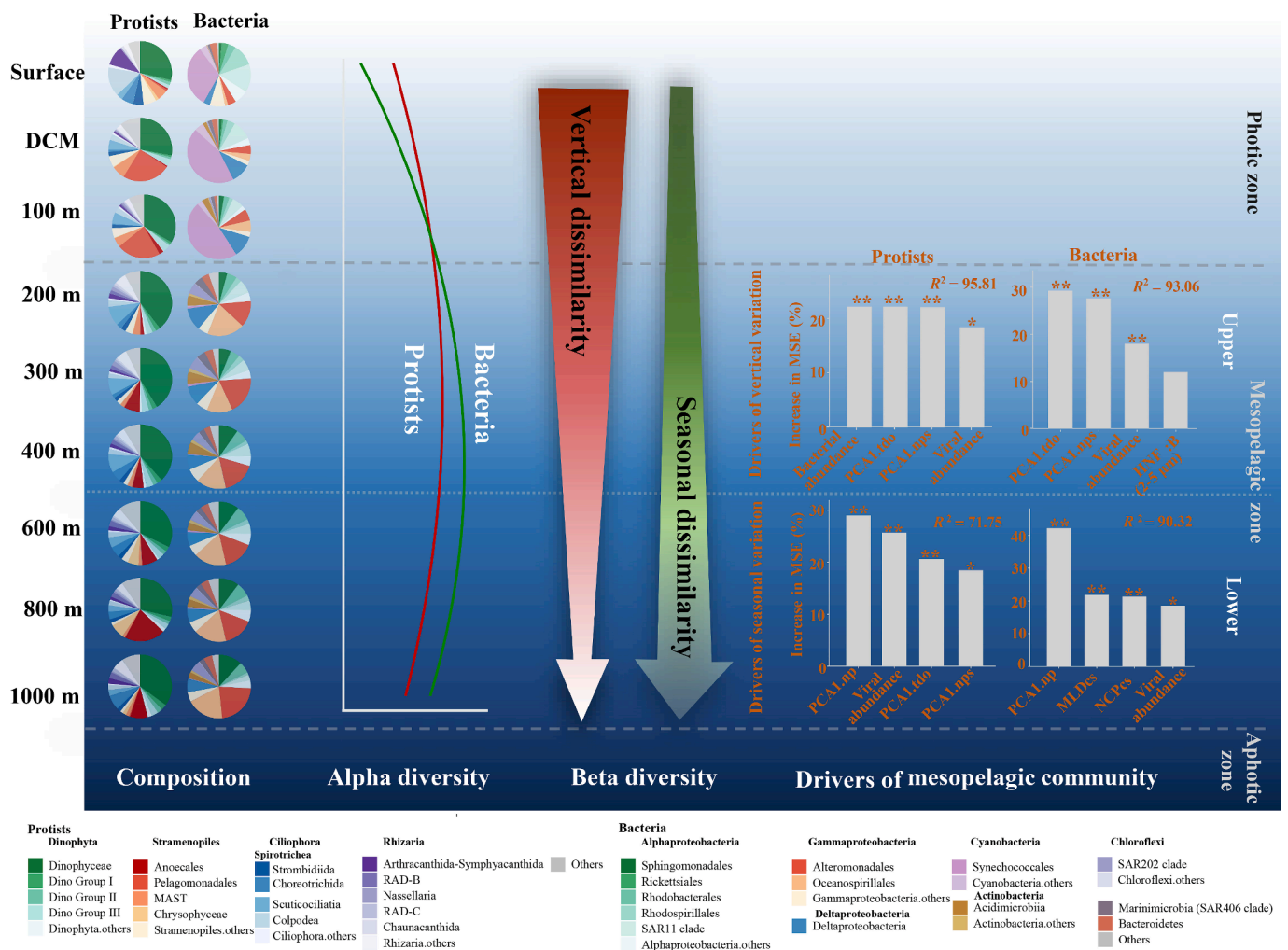
Fig. 6. A conceptual framework for community composition, alpha- and beta-diversity, and underlying drivers influencing the mesopelagic protist-bacteria microbiota in the South China Sea. Left: dynamic shifts in community composition of protists and bacteria across various depth layers, extending from the surface to the mesopelagic zones. Middle two: variations in alpha and beta diversity of protistan and bacterial communities within these specific depth layers. Right: influential factors that govern the vertical and seasonal dynamics of the microbiome within the mesopelagic zones.

that could have appeared to influence the work reported in this paper.].

Data availability

The link has been shared in the manuscript.

Acknowledgements

Appendix A. Supplementary material

Supplementary data to this article can be found online at https://doi.org/10.1016/j.pocean.2024.103280.

References

Aldunate, M., De la Iglesia, R., Bertagnolli, A.D., Ulloa, O., 2018. Oxygen modulates bacterial community composition in the coastal upwelling waters off central Chile. Deep Sea Res. II 156, 68–79. https://doi.org/10.1016/j.dsr2.2018.02.001.

Arandia-Gorostidi, N., Weber, P.K., Alonso-Sáez, L., Morán, X.A.G., Mayali, X., 2017. Elevated temperature increases carbon and nitrogen fluxes between phytoplankton and heterotrophic bacteria through physical attachment. ISME J. 11, 641–650. https://doi.org/10.1038/ismej.2016.156.

Archer, E. 2021. rfPermute: Estimate permutation p-values for random forest importance metrics. https://cran.r-project.org/web/packages/rfPermute/.

Bastian, M., Heymann, S., Jacomy, M., 2009. Gephi: An open source software for exploring and manipulating networks, v0.9.5. Proc. Int. AAAI Conf. Web Soc. Media 3, 361–362.

Behrenfeld, M.J., Falkowski, P.G., 1997. Photosynthetic rates derived from satellite-based chlorophyll concentration. Limnol. Oceanogr. 42, 1–20. https://doi.org/10.4319/lo.1997.42.1.0001.

Blanco-Bercial, L., Parsons, R., Bolaños, L.M., Johnson, R., Giovannoni, S.J., Curry, R., 2022. The protist community traces seasonality and mesoscale hydrographic features in the oligotrophic Sargasso Sea. Front. Mar. Sci. 9, 897140 https://doi.org/10.3389/fmars.2022.897140.

Bolger, A.M., Lohse, M., Usadel, B., 2014. Trimmomatic: a flexible trimmer for Illumina sequence data. Bioinformatics 30, 2114–2120. https://doi.org/10.1093/bioinformatics/btu170.

Boscolo-Galazzo, F., Crichton, K.A., Barker, S., Pearson, P.N., 2018. Temperature dependency of metabolic rates in the upper ocean: A positive feedback to global climate change? Global Planet. Change 170, 201–212. https://doi.org/10.1016/j.gloplacha.2018.08.017.

Breiman, L., A. Cutler, A. Liaw, and M. Wiener 2018. Breiman and Cutler's random forests for classification and regression, 4.6.14.

Brown, J.M., Labonté, J.M., Brown, J., Record, N.R., Poulton, N.J., Sieracki, M.E., Logares, R., Stepanauskas, R., 2020. Single cell genomics reveals viruses consumed by marine protists. Front. Microbiol. 11, 524828 https://doi.org/10.3389/fmicb.2020.524828.

Brown, M.V., Philip, G.K., Bunge, J.A., Smith, M.C., Bissett, A., Lauro, F.M., Fuhrman, J.A., Donachie, S.P., 2009. Microbial community structure in the North Pacific ocean. ISME J. 3, 1374–1386. https://doi.org/10.1038/ismej.2009.86.

Brussaard, C.P.D., 2004. Optimization of procedures for counting viruses by flow cytometry. Appl. Environ. Microbiol. 70, 1506–1513. https://doi.org/10.1128/AEM.70.3.1506-1513.2004.

Buesseler, K.O., et al., 2007. Revisiting carbon flux through the ocean's twilight zone. Science 316, 567–570. https://doi.org/10.1126/science.1137959.

Caporaso, J.G., et al., 2010. QIIME allows analysis of high-throughput community sequencing data. Nat. Methods 7, 335–336.

Cho, B.C., Na, S.C., Choi, D.H., 2000. Active ingestion of fluorescently labeled bacteria by mesopelagic heterotrophic nanoflagellates in the East Sea. Korea. Mar. Ecol. Prog. Ser. 206, 23–32. https://doi.org/10.3354/meps206023.

Church, M.J., Lomas, M.W., Muller-Karger, F., 2013. Sea change: Charting the course for biogeochemical ocean time-series research in a new millennium. Deep Sea Res. II 93, 2–15. https://doi.org/10.1016/j.dsr2.2013.01.035.

Cram, J.A., Chow, C.-E.-T., Sachdeva, R., Needham, D.M., Parada, A.E., Steele, J.A., Fuhrman, J.A., 2015a. Seasonal and interannual variability of the marine bacterioplankton community throughout the water column over ten years. ISME J. 9, 563–580. https://doi.org/10.1038/ismej.2014.153.

Cram, J.A., Xia, L.C., Needham, D.M., Sachdeva, R., Sun, F., Fuhrman, J.A., 2015b. Cross-depth analysis of marine bacterial networks suggests downward propagation of temporal changes. ISME J. 9, 2573–2586. https://doi.org/10.1038/ismej.2015.76.

Dall'Olmo, G., Dingle, J., Polimene, L., Brewin, R.J., Claustre, H., 2016. Substantial energy input to the mesopelagic ecosystem from the seasonal mixed-layer pump. Nat. Geosci. 9, 820–823. https://doi.org/10.1038/ngeo2818.

de Vargas, C., et al., 2015. Eukaryotic plankton diversity in the sunlit ocean. Science 348, 1261605. https://doi.org/10.1126/science.1261605.

Delaney, M., 2003. Effects of temperature and turbulence on the predator–prey interactions between a heterotrophic flagellate and a marine bacterium. Microb. Ecol. 45, 218–225. https://doi.org/10.1007/s00248-002-1058-4.

Dell'Anno, A., Corinaldesi, C., 2004. Degradation and turnover of extracellular DNA in marine sediments: ecological and methodological considerations. Appl. Environ. Microbiol. 70, 4384–4386. https://doi.org/10.1128/aem.70.7.4384-.

DeLong, E.F., et al., 2006. Community genomics among stratified microbial assemblages in the ocean's interior. Science 311, 496–503. https://doi.org/10.1126/science.1120250.

Dolan, J.R., Ciobanu, M., Marro, S., Coppola, L., 2019. An exploratory study of heterotrophic protists of the mesopelagic Mediterranean Sea. ICES J. Mar. Sci. 76, 616–625. https://doi.org/10.1093/icesjms/fsx218.

Du, C., et al., 2013. Impact of the kuroshio intrusion on the nutrient inventory in the upper northern south china sea: insights from an isopycnal mixing model. Biogeosciences 10 (10), 6419–6432. https://doi.org/10.5194/bg-10-6419-2013.

Duret, M.T., Pachiadaki, M.G., Stewart, F.J., Sarode, N., Christaki, U., Monchy, S., Srivastava, A., Edgcomb, V.P., 2015. Size-fractionated diversity of eukaryotic microbial communities in the Eastern Tropical North Pacific oxygen minimum zone. FEMS Microbiol. Ecol. 91, fiv037. https://doi.org/10.1093/femsec/fiv037.

Duret, M.T., Lampitt, R.S., Lam, P., 2020. Eukaryotic influence on the oceanic biological carbon pump in the Scotia Sea as revealed by 18S rRNA gene sequencing of suspended and sinking particles. Limnol. Oceanogr. 65, S49–S70. https://doi.org/10.1002/lno.11319.

Durkin, C.A., Van Mooy, B.A., Dyhrman, S.T., Buesseler, K.O., 2016. Sinking phytoplankton associated with carbon flux in the Atlantic Ocean. Limnol. Oceanogr. 61, 1172–1187. https://doi.org/10.1002/lno.10253.

Edgar, R.C., 2013. UPARSE: highly accurate OTU sequences from microbial amplicon reads. Nat. Methods 10, 996–998. https://doi.org/10.1038/nmeth.2604.

Emerson, S., 2014. Annual net community production and the biological carbon flux in the ocean. Global Biogeochem. Cycles 28, 14–28. https://doi.org/10.1002/2013gb004680.

Flegontova, O., Flegontov, P., Jachníková, N., Lukeš, J., Horák, A., 2023. Water masses shape pico-nano eukaryotic communities of the Weddell Sea. Commun. Biol. 6, 64. https://doi.org/10.1038/s42003-023-04452-7.

Friedlingstein, P., et al., 2022. Global carbon budget 2022. Earth Syst. Sci. Data Discuss. 14, 4811–4900. https://doi.org/10.5194/essd-14-4811-2022.

Fuchs, B.M., Woebken, D., Zubkov, M.V., Burkill, P.H., Amann, R., 2005. Molecular identification of picoplankton populations in contrasting waters of the Arabian Sea. Aquat. Microb. Ecol. 39, 145–157. https://doi.org/10.3354/ame039145.

Fuhrman, J.A., McCallum, K., Davis, A.A., 1993. Phylogenetic diversity of subsurface marine microbial communities from the Atlantic and Pacific Oceans. Appl. Environ. Microbiol. 59, 1294–1302. https://doi.org/10.1128/aem.59.5.1294-1302.1993.

Giner, C.R., Pernice, M.C., Balagué, V., Duarte, C.M., Gasol, J.M., Logares, R., Massana, R., 2020. Marked changes in diversity and relative activity of picoeukaryotes with depth in the world ocean. ISME J. 14, 437–449. https://doi.org/10.1038/s41396-019-0506-9.

Gordon, D., Giovannoni, S., 1996. Detection of stratified microbial populations related to *Chlorobium* and *Fibrobacter* species in the Atlantic and Pacific Oceans. Appl. Environ. Microbiol. 62, 1171–1177. https://doi.org/10.1128/aem.62.4.1171-1177.1996.

Gu, Z., Gu, L., Eils, R., Schlesner, M., Brors, B., 2014. Circlize implements and enhances circular visualization in R. Bioinformatics 30, 2811–2812. https://doi.org/10.1093/bioinformatics/btu393.

Guerrero-Feijóo, E., Nieto-Cid, M., Sintes, E., Dobal-Amador, V., Hernando-Morales, V., Álvarez, M., et al., 2017. Optical properties of dissolved organic matter relate to different depth-specific patterns of archaeal and bacterial community structure in the North Atlantic Ocean. FEMS Microbiol. Ecol. 93, fiw224. https://doi.org/10.1093/femsec/fiw224.

Guillou, L., et al., 2012. The Protist Ribosomal Reference database (PR2): a catalog of unicellular eukaryote small sub-unit rRNA sequences with curated taxonomy. Nucleic Acids Res. 41, D597–D604. https://doi.org/10.1093/nar/gks1160.

Guillou, L., Viprey, M., Chambouvet, A., Welsh, R., Kirkham, A., Massana, R., Scanlan, D.J., Worden, A.Z., 2008. Widespread occurrence and genetic diversity of marine parasitoids belonging to Syndiniales (Alveolata). Environ. Microbiol. 10, 3349–3365. https://doi.org/10.1111/j.1462-2920.2008.01731.x.

Gutiérrez-Rodríguez, A., et al., 2022. Planktonic protist diversity across contrasting Subtropical and Subantarctic waters of the southwest Pacific. Prog. Oceanogr. 206, 102809 https://doi.org/10.1016/j.pocean.2022.102809.

Hansell, D.A., Orellana, M.V., 2021. Dissolved organic matter in the global ocean: a primer. Gels 7, 128. https://doi.org/10.3390/gels7030128.

Hung, C.-C., Gong, G.-C., Santschi, P.H., 2012. ^{234}Th in different size classes of sediment trap collected particles from the Northwestern Pacific Ocean. Geochim. Cosmochim. Acta 91, 60–74. https://doi.org/10.1016/j.gca.2012.05.017.

Jephcott, T.G., Alves-de-Souza, C., Gleason, F.H., Ogtrop, F.V., Sime-Ngando, T., Karpov, S.A., et al., 2016. Ecological impacts of parasitic chytrids, syndiniales, and

perkinsids on populations of marine photosynthetic dinoflagellates. Fungal Ecol. 19, 47–58. https://doi.org/10.1016/j.funeco.2015.03.007.

Lam, P.J., Doney, S.C., Bishop, J.K., 2011. The dynamic ocean biological pump: Insights from a global compilation of particulate organic carbon, CaCO₃, and opal concentration profiles from the mesopelagic. Global Biogeochem. Cycles 25, GB3009. https://doi.org/10.1029/2010gb003868.

Landry, Z., Swan, B.K., Herndl, G.J., Stepanauskas, R., Giovannoni, S.J., 2017. SAR202 genomes from the dark ocean predict pathways for the oxidation of recalcitrant dissolved organic matter. MBio 8, e00413–e417. https://doi.org/10.1128/mbio.00413-17.

Laws, E.A., Falkowski, P.G., Smith Jr, W.O., Ducklow, H., McCarthy, J.J., 2000. Temperature effects on export production in the open ocean. Global Biogeochem. Cycles 14, 1231–1246. https://doi.org/10.1029/1999gb001229.

Laws, E.A., D'Sa, E., Naik, P., 2011. Simple equations to estimate ratios of new or export production to total production from satellite-derived estimates of sea surface temperature and primary production. Limnol Oceanogr: Meth. 9 (12), 593–601. https://doi.org/10.4319/lom.2011.9.593.

Li, T., Bai, Y., He, X., Chen, X., Chen, C.-T.-A., Tao, B., Pan, D., Zhang, X., 2018. The relationship between POC export efficiency and primary production: Opposite on the shelf and basin of the northern South China Sea. Sustainability 10, 3634. https://doi.org/10.3390/su10103634.

Li, H., Wiesner, M.G., Chen, J., Ling, Z., Zhang, J., Ran, L., 2017. Long-term variation of mesopelagic biogenic flux in the central South China Sea: Impact of monsoonal seasonality and mesoscale eddy. Deep Sea Res. I 126, 62–72. https://doi.org/10.1016/j.dsr.2017.05.012.

Long, R.A., Azam, F., 2001. Microscale patchiness of bacterioplankton assemblage richness in seawater. Aquat. Microb. Ecol. 26, 103–113. https://doi.org/10.3354/ame026103.

Magoč, T., Salzberg, S.L., 2011. FLASH: fast length adjustment of short reads to improve genome assemblies. Bioinformatics 27, 2957–2963. https://doi.org/10.1093/bioinformatics/btr507.

Marie, D., Partensky, F., Vaulot, D., Brussaard, C., 1999. Enumeration of phytoplankton, bacteria, and viruses in marine samples. Curr. Protoc. Cytom. Chapter 11: Unit 11.11. https://doi.org/10.1002/0471142956.cy1111s10.

Mestre, M., Ruiz-González, C., Logares, R., Duarte, C.M., Gasol, J.M., Sala, M.M., 2018. Sinking particles promote vertical connectivity in the ocean microbiome. Proc. Natl. Acad. Sci. 115, E6799–E6807. https://doi.org/10.1073/pnas.1802470115.

Morris, R., Rappé, M., Urbach, E., Connon, S., Giovannoni, S., 2004. Prevalence of the Chloroflexi-related SAR202 bacterioplankton cluster throughout the mesopelagic zone and deep ocean. Appl. Environ. Microbiol. 70, 2836–2842. https://doi.org/10.1128/aem.70.5.2836-2842.2004.

Oksanen, J. F., G. Blanchet, R. Kindt, P. Legendre, R. G. O'Hara, L. G. Simpson, and J. Weedon. 2010. Vegan: community ecology package. R package version 1.17-4. http://CRAN.R-project.org/package=vegan.

Ollison, G.A., Hu, S.K., Mesrop, L.Y., DeLong, E.F., Caron, D.A., 2021. Come rain or shine: depth not season shapes the active protistan community at station ALOHA in the North Pacific Subtropical Gyre. Deep Sea Res. I 170, 103494. https://doi.org/10.1016/j.dsr.2021.103494.

Orcutt, B., Sylvan, J., Knab, N., Edwards, K., 2011. Microbial ecology of the dark ocean above, at, and below the seafloor. Microbiol. Mol. Biol. Rev. 75 (2), 361–422. https://doi.org/10.1128/mmbr.00039-10.

Orsi, W.D., Smith, J.W., Liu, S., Liu, Z., Sakamoto, C.M., Wilken, S., et al., 2016. Diverse, uncultivated bacteria and archaea underlying the cycling of dissolved protein in the ocean. ISME J. 10 (9), 2158–2173. https://doi.org/10.1038/ismej.201.

Orsi, W., Song, Y.C., Hallam, S., Edgcomb, V., 2012. Effect of oxygen minimum zone formation on communities of marine protists. ISME J. 6, 1586–1601. https://doi.org/10.1038/ismej.2012.7.

Pachiadaki, M.G., Taylor, C., Oikonomou, A., Yakimov, M.M., Stoeck, T., Edgcomb, V., 2016. In situ grazing experiments apply new technology to gain insights into deep-sea microbial food webs. Deep Sea Res. II 129, 223–231. https://doi.org/10.1016/j.dsr2.2014.10.019.

Parsons, T.R., Maita, Y.R., Lalli, C.M., 1984. A manual of chemical & biological methods for seawater analysis. Pergamin Press, p. (p. 173)..

Pernice, M.C., et al., 2015. Global abundance of planktonic heterotrophic protists in the deep ocean. ISME J. 9, 782–792. https://doi.org/10.1038/ismej.2014.168.

Quast, C., Pruesse, E., Yilmaz, P., Gerken, J., Schweer, T., Yarza, P., Peplies, J., Glöckner, F.O., 2012. The SILVA ribosomal RNA gene database project: improved data processing and web-based tools. Nucleic Acids Res. 41, D590–D596. https://doi.org/10.1093/nar/gks1219.

Rigonato, J., et al., 2023. Ocean-wide comparisons of mesopelagic planktonic community structures. ISME Commun. 3, 83. https://doi.org/10.1038/s43705-023-00279-9.

Robinson, C., et al., 2010. Mesopelagic zone ecology and biogeochemistry–a synthesis. Deep Sea Res. II 57, 1504–1518. https://doi.org/10.1016/j.dsr2.2010.02.018.

Rocke, E., Pachiadaki, M.G., Cobban, A., Kujawinski, E.B., Edgcomb, V.P., 2015. Protist community grazing on prokaryotic prey in deep ocean water masses. PLoS One 10, e0124505.

Roggenbuck, M., et al., 2014. The microbiome of New World vultures. Nat. Commun. 5, 5498. https://doi.org/10.1038/ncomms6498.

Ruiz-González, C., et al., 2020. Major imprint of surface plankton on deep ocean prokaryotic structure and activity. Mol. Ecol. 29, 1820–1838. https://doi.org/10.1111/mec.15454.

Salazar, G., Cornejo-Castillo, F.M., Benítez-Barrios, V., Fraile-Nuez, E., Álvarez-Salgado, X.A., Duarte, C.M., et al., 2016. Global diversity and biogeography of deep-sea pelagic prokaryotes. ISME J. 10 (3), 596–608. https://doi.org/10.1038/ismej.2015.137.

Sarmento, H., Montoya, J.M., Vázquez-Domínguez, E., Vaqué, D., Gasol, J.M., 2010. Warming effects on marine microbial food web processes: how far can we go when it comes to predictions? Philos. Trans. r. Soc. B 365, 2137–2149. https://doi.org/10.1098/rstb.2010.0045.

Shea, C., Wojtal, P., Close, H., Maas, A., Stamieszkin, K., Cope, J., et al., 2023. Small particles and heterotrophic protists support the mesopelagic zooplankton food web in the subarctic northeast pacific ocean. Limnol. Oceanogr. 68 (8), 1949–1963. https://doi.org/10.1002/lno.12397.

Sherr, E.B., Caron, D.A., and B.F. Sherr. 1993. Staining of heterotrophic protists for visualization via epifluorescence microscopy. Handbook of Methods in Aquatic Microbial Ecology, pp. 213-227.

Šimek, K., Hartman, P., Nedoma, J., Pernthaler, J., Springmann, D., Vrba, J., et al., 1997. Community structure, picoplankton grazing, and zooplankton control of heterotrophic nanoflagellates in a eutrophic reservoir during the summer phytoplankton maximum. Aquat. Microb. Ecol. 12, 49–63. https://doi.org/10.3354/ame012049.

St. John, M.A., Borja, A., Chust, G., Heath, M., Grigorov, I., Mariani, P., Martin, A.P., Santos, R.S., 2016. A dark hole in our understanding of marine ecosystems and their services: perspectives from the mesopelagic community. Front. Mar. Sci. 3, 31. https://doi.org/10.3389/fmars.2016.00031.

Steinberg, D.K., Van Mooy, B.A., Buesseler, K.O., Boyd, P.W., Kobari, T., Karl, D.M., 2008. Bacterial vs. zooplankton control of sinking particle flux in the ocean's twilight zone. Limnol. Oceanogr. 53, 1327–1338. https://doi.org/10.4319/lo.2008.53.4.1327.

Stoeck, T., Bass, D., Nebel, M., Christen, R., Jones, M.D., Breiner, H.W., Richards, T.A., 2010. Multiple marker parallel tag environmental DNA sequencing reveals a highly complex eukaryotic community in marine anoxic water. Mol. Ecol. 19, 21–31. https://doi.org/10.1111/j.1365-294x.2009.04480.x.

Sun, P., et al., 2019. Integrated space-time dataset reveals high diversity and distinct community structure of ciliates in mesopelagic waters of the northern South China Sea. Front. Microbiol. 10, 2178. https://doi.org/10.3389/fmicb.2019.02178.

Sun, P., Wang, Y., Zhang, Y., Logares, R., Cheng, P., Xu, D., Huang, B., 2023. From the sunlit to the aphotic zone: assembly mechanisms and co-occurrence patterns of protistan-bacterial microbiotas in the western pacific ocean. mSystems 8, e00013–e00023. https://doi.org/10.1128/msystems.00013-23.

Sunagawa, S., et al., 2015. Structure and function of the global ocean microbiome. Science 348, 1261359. https://doi.org/10.1126/science.1261359.

Tanaka, T., Rassoulzadegan, F., 2004. Vertical and seasonal variations of bacterial abundance and production in the mesopelagic layer of the nw mediterranean sea: bottom-up and top-down controls. Deep Sea Res. Part I Oceanogr. Res. Pap. 51 (4), 531–544. https://doi.org/10.1016/j.dsr.2003.12.001.

Thrash, J. C., K. W. Seitz, B. J. Baker, B. Temperton, L. E. Gillies, N. N. Rabalais, B. Henrissat, and O. U. Mason. 2017. Metabolic roles of uncultivated bacterioplankton lineages in the northern Gulf of Mexico "Dead Zone". MBio 8: 10.1128/mbio. 01017-01017. doi:10.1128/mbio.01017-17.

Trombetta, T., Vidussi, F., Roques, C., Mas, S., Scotti, M., Mostajir, B., 2021. Co-occurrence networks reveal the central role of temperature in structuring the plankton community of the Thau Lagoon. Sci. Rep. 11, 17675. https://doi.org/10.1038/s41598-021-97173-y.

Ulloa, O., Canfield, D.E., DeLong, E.F., Letelier, R.M., Stewart, F.J., 2012. Microbial oceanography of anoxic oxygen minimum zones. Proc. Natl. Acad. Sci. 109, 15996–16003. https://doi.org/10.1073/pnas.1205009109.

Urrutxurtu, I., Orive, E., de la Sota, A., 2003. Seasonal dynamics of ciliated protozoa and their potential food in an eutrophic estuary (Bay of Biscay). Estuar. Coast. Shelf Sci. 57, 1169–1182. https://doi.org/10.1016/s0272-7714(03)00057-x.

Wright, J.J., Konwar, K.M., Hallam, S.J., 2012. Microbial ecology of expanding oxygen minimum zones. Nat. Rev. Microbiol. 10, 381–394. https://doi.org/10.1038/nrmicro2778.

Wright, T.D., Vergin, K.L., Boyd, P.W., Giovannoni, S.J., 1997. A novel delta-subdivision proteobacterial lineage from the lower ocean surface layer. Appl. Environ. Microbiol. 63, 1441–1448. https://doi.org/10.1128/aem.63.4.1441-1448.1997.

Xiao, W., Wang, L., Laws, E., Xie, Y., Chen, J., Liu, X., Chen, B., Huang, B., 2018. Realized niches explain spatial gradients in seasonal abundance of phytoplankton groups in the South China Sea. Prog. Oceanogr. 162, 223–239. https://doi.org/10.1016/j.pocean.2018.03.008.

Yamada, Y., Tomaru, Y., Fukuda, H., Nagata, T., 2018. Aggregate formation during the viral lysis of a marine diatom. Front. Mar. Sci. 5, 167. https://doi.org/10.3389/fmars.2018.00167.

Yang, W., Zhao, X., Zheng, M., 2022. Slow-sinking particulate organic carbon and its attenuation in the mesopelagic water of the South China Sea. Front. Mar. Sci. 9, 1018825. https://doi.org/10.3389/fmars.2022.1018825.

Yilmaz, P., Yarza, P., Rapp, J.Z., Glöckner, F.O., 2016. Expanding the world of marine bacterial and archaeal clades. Front. Microbiol. 6, 1524. https://doi.org/10.3389/fmicb.2015.01524.

Zhao, H., Zhang, Z., Nair, S., Zhao, J., Mou, S., Xu, K., Zhang, Y., 2022. Vertically Exported Phytoplankton (< 20 μm) and Their Correlation Network With Bacterioplankton Along a Deep-Sea Seamount. Front. Mar. Sci. 9, 862494 https://doi.org/10.3389/fmars.2022.862494.

Zinger, L., Gobet, A., Pommier, T., 2012. Two decades of describing the unseen majority of aquatic microbial diversity. Mol. Ecol. 21, 1878–1896. https://doi.org/10.1111/j.1365-294x.2011.05362.x.

Zoccarato, L., Pallavicini, A., Cerino, F., Umani, S.F., Celussi, M., 2016. Water mass dynamics shape Ross Sea protist communities in mesopelagic and bathypelagic layers. Prog. Oceanogr. 149, 16–26. https://doi.org/10.1016/j.pocean.2016.10.003.